Ramadan and Elgendi
Journal of Engineering and Applied Science (2023) 70:61
https://doi.org/10.1186/s44147-023-00209-5

Journal of Engineering and Applied Science

REVIEWS Open Access

A review of optimization techniques and algorithms used for FRP applications in civil engineering

Amany S. Ramadan[1*] and Elbadr O. Elgendi[1*]

*Correspondence: Amany.Ramadan7@student.aast.edu; elbadrosman@aast.edu

[1] Construction and Building Engineering Department, College of Engineering and Technology, Arab Academy for Science, Technology and Maritime Transport (AASTMT), Alexandria, Egypt

Abstract

Optimization problems aim to minimize or maximize an objective function while fulfilling related constraints. This objective function may be a single or multi-objective optimization. Many studies have been conducted on using these optimization problems in civil and construction engineering, especially for the various machine learning techniques and algorithms that have been developed for fiber reinforced polymer (FRP) applications in the rehabilitation and design of RC structures. FRP is considered the most effective and superior technique for strengthening and retrofitting due to its significant benefits over traditional methods, which have numerous drawbacks, as well as the importance of structural strengthening as a cost-effective and practical option. In this research, an insight into how to apply algorithms and machine learning approaches to optimize FRP applications in civil and construction engineering is presented, as well as a detailed analysis of the various optimization strategies used and their findings. A total of 18 case studies from previous research were discussed and critically evaluated, and they were categorized into six groups according to the algorithm or machine learning technique utilized. Based on the case studies investigated in this study, the genetic algorithm was found to be the optimal algorithm utilized for optimizing FRP applications. The result of this research provides a useful guideline for future researchers and specialists.

Keywords: FRP, Optimization, Algorithms, Machine learning, Strengthening

Introduction

Fiber reinforced polymer (FRP) composites are gaining popularity in design and strengthening technologies. Due to their superior strength-to-weight ratio and flexibility to customize their properties to meet complex requirements, FRP has been applied in various structural applications for nearly 80 years since WWII. FRP offers several advantages that encourage engineers to utilize it in complex applications, such as the ability to strengthen or repair existing structures, rehabilitating the performance and efficiency of damaged structures, reinforcing any element in any shape and orientation, and being moldable into complex shapes with a high weight-to-strength ratio and minimal maintenance requirements. Furthermore, FRP can be applied without putting the structure's

operation on hold or losing time or function. FRP is also resilient to environmental factors and can withstand the corrosive effects of harsh environments. FRP has successfully strengthened structures that are not ductile enough to sustain earthquake forces and those that do not meet new standards and requirements [1–3]. There are various types of FRP composites, each with distinct mechanical characteristics. Glass FRP (GFRP), aramid FRP (AFRP), carbon FRP (CFRP), and basalt FRP are frequently used types in the literature and are employed for strengthening RC elements for common applications such as flexural and shear. The use of these types helps to develop design standards for further FRP-RC applications, in addition to maintaining the safety and functionality of RC members [4–9].

The practice of strengthening reinforced concrete (RC) structures from the outside has become popular over the past few decades in both scientific and industrial communities. In this application, composite materials are adhered to the surfaces of RC members to make them stronger, stiffer, and more flexible. For instance, to increase the shear capacity of RC beams, FRP wraps and strips can be externally bonded (EB) with epoxy. The main shear-strengthening systems that are most frequently discussed in the literature are FRP side-bonded and U-wrapped sheets and strips. Seismic strengthening of RC structures using FRP jackets, especially when used to restrict RC columns, can considerably improve the columns' ductility and strength, making it one of the most crucial retrofitting techniques for improving their seismic performance [10–15]. Additionally, the near-surface mounting (NSM) technique is used to insert FRP composites into the concrete cover for strengthening purposes, either as bars or strips. This technique is preferred over externally bonded (EB) methods due to its significant increase in load capacity and reduction of the breakdown of FRP/concrete bonds. Flexural retrofitting of RC beams is one of the widely used applications for NSM-FRP strengthening, as cited in references [4, 16]. In the context of designing concrete members, fiber-reinforced polymer (FRP) bars are gaining increasing attention as a suitable substitute for traditional steel bars due to their resistance to corrosion, particularly in marine and coastal engineering. FRP bars have numerous applications in columns, beams, and slabs [17–22]. The use of FRP in designing and strengthening structures should be evaluated to optimize its design and cost while meeting the criteria of relevant codes, standards, and experimental data, given its substantial benefits against static and dynamic loads.

The optimal option from among all conceivable options in a pool of alternatives is defined as an optimization problem. The optimization technique is a useful tool for selecting the ideal operational conditions and design characteristics. Optimization is the process of identifying the values of the choice variables that produce the maximal or minimal outcome for one or more defined objectives. The choice of target functions and optimization method affects how reliable optimal solutions are. Optimization search may be used to estimate unknowable parameters in complex nonlinear processes. Multiphase reactors and flow systems could benefit from optimization to help them scale up. Computer-assisted decision-making is an attempt to provide high-tech assistance to the decision-making process. Through algorithms and machine learning approaches, computers are now utilized to both analyze the model and search for improved operating conditions. Variables, objectives, and constraints are the components of an optimization problem [23]. Over the last two decades, algorithms have been used to deal with a

variety of engineering optimization problems and have contributed immensely to solving several specific types of civil engineering challenges [24].

The optimization problem for FRP used in designing or strengthening RC structures involves selecting the right sizes for FRP sheets and laminates for flexural and shear strengthening. Therefore, the goal of sizing optimization is to maintain design restrictions while minimizing the cost of the proposed system for repairing structures. The evaluation of FRP's use in strengthening and repairing structures is due to its significant benefits against static and dynamic loads by using optimization techniques and algorithms. It considers the requirements of relevant codes and standards as constraints and the need to optimize its design and cost as an objective function. Several optimization algorithms and machine learning techniques have been utilized to solve civil engineering challenges, specifically for FRP applications. Numerous algorithms and machine learning techniques, including single and ensemble models, have been employed to optimize or forecast FRP applications with concrete components for various purposes such as shear, flexure, seismicity, and corrosion. These algorithms include the genetic algorithm (GA) [8, 10, 11, 20, 25], while the ML techniques include the support vector machine (SVM) and the extreme gradient boosting (xgBoost) for the single model and the ensemble model, respectively [26–30].

The optimization algorithms and machine learning techniques mentioned in this research include genetic algorithm (GA), particle swarm optimization (PSO), generalized regression neural network (GRNN), resilient back-propagating neural network (RBPNN), multiple linear regression (MLR), support vector machine (SVM), artificial neural network (ANN), kernel ridge regression (KRR), K-nearest neighbors (KNN), decision trees (CART), random forest (RF), extremely randomized trees (ERT), gradient-boosted trees (GBT), adaptive boosting (AdaBoost), and extreme gradient boosting (xgBoost). The FRP applications mentioned in this research for designing and strengthening RC structures include shear, flexure, and seismic forces, as well as other prediction purposes such as structural health monitoring, corrosion deterioration, and calculation of bond strength between FRP and concrete.

Based on the aforementioned, to further develop and validate the current algorithms and machine learning approaches for optimizing FRP applications in strengthening and designing concrete members such as beams, slabs, and columns against shear, flexure, seismic, corrosion, and other crucial applications, an overview of how to use these techniques in the aforementioned applications is provided. This is accompanied by a thorough analysis of the various optimization strategies employed and their results. The optimal technique is then presented based on the case studies investigated to serve as an effective roadmap for upcoming researchers and specialists.

A review of algorithms and machine learning techniques used for optimizing the FRP current applications

An overview of case studies from 2007 to 2023, which were chosen to approximately cover the most prevalent FRP applications and various optimization strategies and algorithms utilized in optimizing FRP, could be grouped into 6 categories (summarized later).

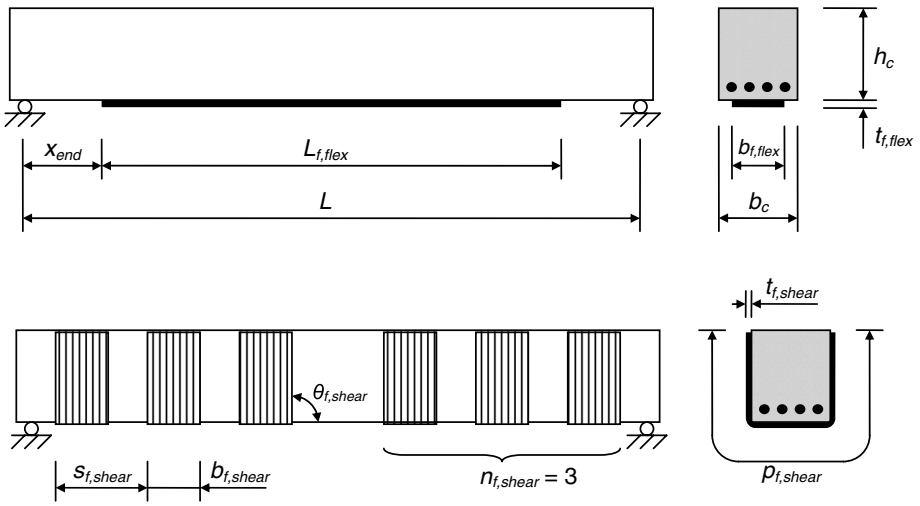

Fig. 1 Strengthening system for shear and flexure [31]

Genetic algorithm (GA) in optimization of FRP

In this subsection, case studies from the literature are presented to discuss the genetic algorithms used to optimize FRP (fiber reinforced polymer) utilized in the design or retrofitting of RC (Reinforced Concrete) structures in shear, flexure, seismic, and corrosion. In 2007, Perera and Varona developed a research study for minimizing the retrofitting cost for RC beams against shear and flexural forces using a genetic algorithm while satisfying design code requirements depending on the limit-states-design criteria (Eurocode 2 in conjunction with the International Federation of Structural Concrete FIB). The strengthening systems are shown in Fig. 1, and the amount of FRP material, surface preparation, and adhesive needed were all factors in determining the cost. The carbon fiber reinforced polymer (CFRP) design optimization example of the GA-based optimization routine was run on MATLAB as presented in Figs. 2 and 3. The original beam capacity was 91.1 kN.m in flexure and 80.5 kN in shear. The capacity needed after increasing the loads on the beam was 123 kN.m in flexure and 115.5 kN in shear. Retrofitting of the beam was required. The findings could be concluded as follows: The configuration of FRP strengthening shown in Table 1 had a capacity of 183 kN.m in flexure and 207 kN in shear. Despite the excessive amount of shear reinforcement, it is the minimum required design for providing resistance against shear in the beam. The design of the bottom plate was determined by the occurrence of interfacial debonding at the plate's end, rather than the maximum applied moment. By following the proposed procedure, the material cost is minimized. The algorithm utilized for this design was simple, systematic, and automated [31].

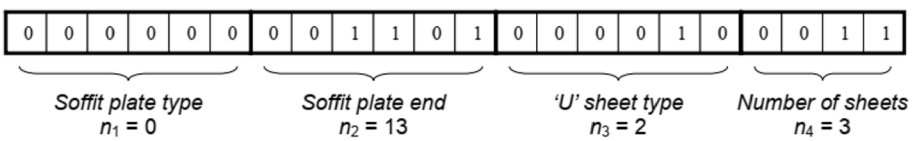

Fig. 2 An example of the chromosome [31]

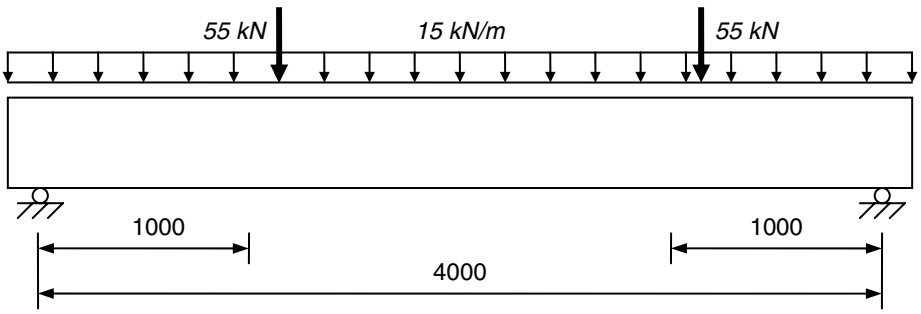

Fig. 3 Application example [31]

Table 1 Optimum strengthening scheme results [31]

GA data: **Population size: 400 / Chromosome size: 22 / Uniform crossover / Crossover prob: 85% / Mutation prob: 10%**				
CFRP for flexure		**CFRP for shear**		**Constraints**
Type	**Length**	**Type**	**Number**	
$t_f = 1.2$ mm (1 ply) $b_f = 3$x80 mm $E_f = 165$ MPa	2813 mm	$t_f = 1$ mm(1 ply) $b_f = 300$ mm $s_f = 650$ mm $\varphi_f = 45°$	2(+2)	None violated

Regarding the preceding case study, despite the author's claim that the proposed technique reduces retrofitting costs, no cost was provided in the research, either before or after the algorithm was used. Furthermore, the results demonstrated the effectiveness of FRP in retrofitting, as the capacity increased and exceeded the required capacity, but they did not demonstrate the effectiveness of the algorithm, as the capacity was determined only after using the algorithm and was not compared to the capacity determined by manual or other methods. Therefore, to gain a better understanding of the potential impact of the suggested technique, it is necessary to compare the findings with results from experimental testing, as well as to illustrate the reduction percentage as compared to manual methods or other approaches.

As an extension of their previous research, Perera and Varona (2009) [32] conducted a study aimed at minimizing the retrofitting costs for RC beams against shear and flexure forces using a genetic algorithm. The study aimed to satisfy design code requirements based on limit-states-design criteria for the ultimate and the workability limit criteria based on the Eurocode (2) in conjunction with FIB (The International Federation for Structural Concrete). The cost determination included the amount of FRP material, preparation of the surface, and the quantity of adhesive needed. The manufacturers' market size data was used to create databases for various FRP setups. The study presented two examples: the first situation required flexural reinforcement while shear reinforcement was used to prevent concrete cover rupture failure, and the second case required both flexure and shear reinforcement. For the first example, two approaches based on the de-bonding limit criterion were utilized: A and B. The original capacity of the RC beam in flexure was 572 kNm and in shear was 306.9 kN, while the required capacity in flexure was 698.6 kNm and in shear was 266.6 kN. The GA algorithm was applied to both

approaches, and then updated to include the Jansze 1997 model, which was utilized in conjunction with both approaches A and B to conduct a comparison study. The Matthys 2000 model was used to evaluate ripping off at flexural fractures with approach (B) for flexural strengthening, and the Jansze 1997 model was used to assess plate end rupture failure in the second example. The original capacity of the beam was 129.6 kNm in flexure and 67.3 kN in shear, while the required capacity was 189.3 kNm in flexure and 124.3 kN in shear. The findings of the study were as follows: in the first example, when comparing approach (A) to the Jansze 1997 model, the same optimal length for flexural strengthening was achieved while the optimal plates were less than those resulting from the Jansze 1997 model. The shear force was greater than the shear resistance at the plate end, as predicted by Jansze's model. Tables 2 and 4 discuss the results. As a result, the GA optimization technique provided U-shaped jacketed sheets to prevent rupture failure for the concrete cover by acting as a mechanical pillar for the CFRP plate end, whereas strategy (B) resulted in the same optimal plates and a relatively long flexural panel, which increased shear resistance for panels that ended extremely near to the supports, as shown in Tables 3 and 4. Therefore, this method did not require the use of U-sheets. In the second example, Table 5 and Fig. 4 illustrated the optimal configuration in shear and flexure. The algorithm proved to be straightforward, methodical, and automated [32].

Table 2 Approach A (100 Runs) First example [32]

z calculated through...	Average of generations	Optimum CFRP plate	Optimum length (m)	Optimum cost	Average computing time (s)
Linear elastic analysis	16.5	3 x 812 S	4.74	2,051.5	1.69
Approximated expression	17.3	3 x 812 S	4.21	1,822.2	1.75
Nonlinear analysis	17.1	3 x 812 S	4.20	1,817.9	1.75

Table 3 Approach B (100 Runs) First example [32]

z calculated through.	Average of generations	Optimum CFRP plate	Optimum length (m)	Optimum cost
Linear elastic analysis	16.0	4 x 812 M	8.47	5,313.4
Approximated expression	15.7	4 x 812 M	8.46	5,307.1
Nonlinear analysis	15.5	4 x 812 M	8.46	5,307.1

Table 4 Jansze's Model (1997) - Optimum designs (100 Runs) First example [32]

Approach	Average of generations	Optimum CFRP plate	Optimum length (m)	Optimum CFRP sheet	Optimum number of U-sheets	Optimum cost
A	17.8	4 x 812 S	4.21	1 ply/90^0	4, spaced 400 mm	3,740.1
B	15.9	4 x 812 M	8.86	-	-	5,558.0

Table 5 Second example—Optimum design result [32]

CFRP for flexure		CFRP for shear	
Type	**Length**	**Type**	**Number**
$t_{f,flex} = 2.4$ mm (2 plies) $b_{f,flex} = 2$ x 80 mm $E_{f,flex} = 210$ GPa	5.63 m	$t_{f,shear} = 1$ mm (1 ply) $b_{f,shear} = 300$ mm $S_{f,shear} = 700$ mm	3(+3)

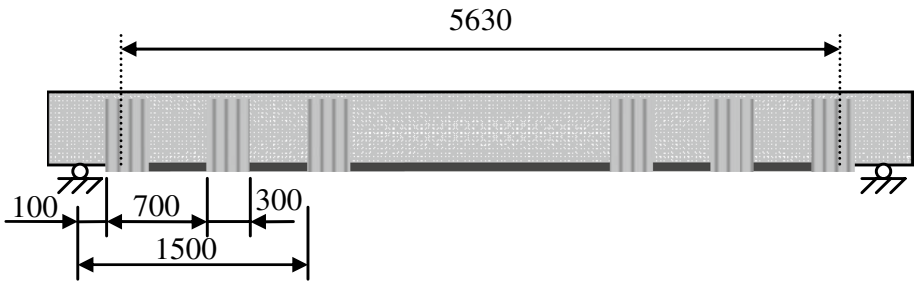

Fig. 4 Second example—optimal scheme [32]

Regarding the preceding case study, for the first example, it was useful to compare the algorithm's results with those of the Jansze model (1997) after integrating them with the algorithm. This comparison showed that the GA model produced the best configuration at a lower cost than those of the Jansze model (1997), along with an illustration of the FRP configuration and cost for each case. However, it was also desirable to demonstrate the effectiveness of FRP in increasing capacity by showing the retrofitted capacity for each case. For the second case, it would be beneficial to clarify the algorithm's success by indicating the retrofitting capacity and cost. Furthermore, the datasets used for FRP configurations included market size values provided by the manufacturer, which brought solutions closer to reality and made them useful in real-world applications. However, it is preferable to compare the findings with those of experimental testing or manual solutions to ensure that the algorithm used for optimizing cost was accurate and to preserve the reality of the results.

Furthermore, in 2007, M. Nehdi et al. performed a study on concrete beams that were reinforced with FRP and optimized their ability to resist shear using a genetic algorithm. The primary aim of the genetic algorithm was to minimize the difference between the monitored and calculated values of shear strength for the FRP-reinforced concrete beams. This involved developing equations using the genetic algorithm that could accurately predict the shear strength values of the FRP-reinforced concrete beams, which were closest to the values that were obtained through experimental testing. Two sets of beams were used, with and without stirrups. The final settings for the GA in both models were as follows: for the beam set without stirrups, there were 70 individuals, a maximum generation size of 1000, a recombination rate of 0.5, and a mutation rate of 0.01, whereas for the beam set with stirrups, there were 100 individuals, a maximum generation size of 5000, a recombination rate of 0.75, and a mutation rate of 0.001. Comparative studies were conducted using the experimental data as well as commonly used codes and standards, as mentioned in Table 6. The comparison terms were the average, coefficient of variation (COV) for Vm/Vcal, standard

Table 6 Shear design equations performance [17]

Method	Without shear reinforcement (50 beams)				With shear reinforcement (100 beams)			
	AAE (%)	V measured / V calculated			AAE (%)	V measured / V calculated		
		Average	SD	COV (%)		Average	SD	COV (%)
ACI 440.1 R-03	68.35	4.02	2.11	52	45.57	1.90	0.91	47
ACI 440.1 R-06	29.74	1.51	0.69	45	31.33	1.22	0.48	39
CSA S806-02	33.13	1.68	0.66	39	17.49	1.13	0.27	24
JSCE-97	33.16	1.69	0.71	41	50.05	2.22	0.73	32
ISIS Canada-01	34.57	1.69	0.81	48	29.52	1.06	0.33	31
Proposed equations	22.42	1.35	0.45	33	19.10	1.23	0.33	26

deviation (SD), and the average absolute error (AAE). The following is a summary of the findings: when analyzing the shear capacity of FRP-reinforced concrete beams that have no shear reinforcement, all shear principles discussed in this study provided unduly conservative conclusions. With a low elastic modulus, the ACI 440 equation was acceptable for predicting the FRP stirrup capacity; however, the nominal shear strength of concrete beams reinforced by FRP stirrups became overly optimistic with a highly elastic modulus, overstating the capacity of FRP stirrup. For low shear strength beams, the JSCE-97 shear provisions produced a reasonably precise estimation of the shear strength given by reinforcement with FRP stirrups. For beams with a large shear capacity, however, such precautions were quite cautious. The proposed procedure achieved the target in good agreement with the experimental data and proved that the genetic algorithm is an effective tool, and the code's recommendations are more conservative, as compared in Table 6 [17].

In discussing the prior case study, the success of the algorithm in optimizing shear design is demonstrated by comparing its results with four widely used codes and standards, namely JSCE, CSA S806, ISIS Canada, and ACI 440. Additionally, the use of experimental data allows for the verification of the algorithm's results, bringing them closer to reality and making them useful in real-world applications. However, it would be preferable to include the schematic configuration of the beams, showing their dimensions and reinforcing details, as well as an example that offers the shear capacity from experimental, codes, and algorithm as values. This will make the comparison more obvious and facilitate further verification.

Additionally, in 2010 Nehdi and Nikopour presented a framework for optimizing the shear resistance of reinforced concrete beams that are externally bonded with fiber-reinforced polymer (FRP) by utilizing genetic algorithms. The geometrical properties of the chosen beam are shown in Fig. 5. Comparative studies were conducted with experimental data from literature as well as commonly used codes and models. The ultimate shear capacities of 212 beams bonded externally with various types of FRP were gathered from the literature. The proposed shear design equations in this paper take into account the shear span-to-thickness ratio, as well as the interaction between concrete, FRP laminates, and steel stirrups, resulting in more precise predictions. Furthermore, the model

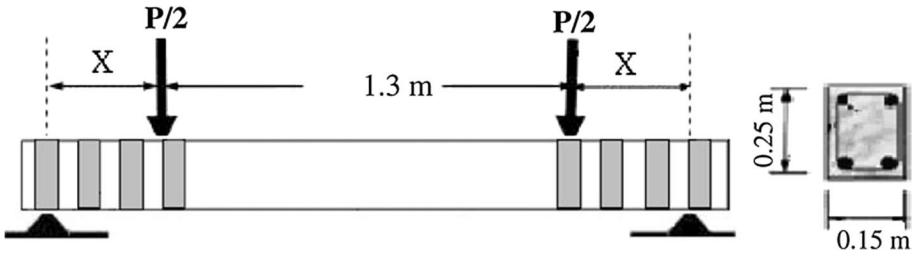

Fig. 5 Geometrical properties of the chosen beam [7]

contains coefficients C1 and C2, which relate to aggregate interlock effect and longitudinal rebars effect, respectively, as well as coefficients C3 and C4, which relate to the final strain level in FRP sheets. The proposed model performance was investigated using the experimental records mentioned before and then validated with a new set of test data collected from literature for 21 beams. The following is a summary of the findings: The shear equation developed using the GAs methodology surpassed the other models taken into consideration in this investigation. It also offered more accurate shear predictions, as shown in Tables 7 and 8, which compare the average, standard deviation SD, coefficient of variation COV for V_m/V_{cal}, and the average absolute error AAE. The ACI 440 method does not take into account how the shear span-to-depth ratio affects the effective shear strain in FRP laminates. The Matthys model does not consider the interaction between concrete, steel, and FRP laminates in its calculations. Similarly, the Colotti model disregards both of these factors in its approach. By improving the containment of

Table 7 Results for the original collected set [7]

Method	AAE (%)	V exp / V cal		
		Average	SD	COV (%)
ACI-440. 2R-02	59.8	1.62	0.52	33.0
CSA S806-02	52.5	1.56	0.43	27.0
ISIS Canada	46.3	1.43	0.38	27.0
Eurocode (EC2)	27.2	0.91	0.20	22.4
Matthys	29.3	0.94	0.24	26.2
Colotti	22.3	1.08	0.18	17.0
Proposed equation	16.5	1.00	0.15	15.0

Table 8 Results for new collected set [7]

Method	AAE (%)	V exp / V cal		
		Average	SD	COV (%)
ACI-440. 2R-02	58.6	1.64	0.49	29.9
CSA S806-02	55.3	1.59	0.45	28.3
ISIS Canada	52.2	1.53	0.39	25.5
Eurocode (EC2)	24.2	0.92	0.21	22.8
Matthys	23.3	0.94	0.25	26.6
Colotti	22.7	1.06	0.19	17.9
Proposed equation	18.9	1.05	0.17	16.1

the reinforced concrete beam, which results in the aggregate interlock, the completely wrapped design outperforms previous methods for shear retrofitting of reinforced concrete beams. Moreover, it provides an improved bonding capability between FRP and concrete. When using a fully wrapped configuration, the C1 coefficient for CFRP was 16% higher compared to a two- or three-sided bonded application, and it was higher than the C1 coefficients for GFRP and AFRP by 10% and 20%, respectively. In addition, CFRP had the greatest C3 and minimal C4 coefficients when compared to GFRP and AFRP. As a result, CFRP composites provide greater shear resistance for retrofitting RC beams with completely wrapped systems, and these composites provide better shear capacity than aramid fiber reinforced polymer (AFRP) or glass fiber reinforced polymer (GFRP). The proposed procedure achieved the target in good agreement with experimental data [7].

Analyzing the preceding case study, comparing the algorithm's output to Eurocode (EC2), ACI 440, CSA 860, ISIS Canada recommendations, the Matthys Model, and Colotti Model was significant, as it shows the success of the algorithm in optimizing shear design. Additionally, the use of experimental data and the new set of beams allows for the verification of the algorithm's results, bringing them closer to reality and making them useful in real-world applications. Furthermore, diverse forms of FRP (carbon, glass, and aramid) were used in the case study, highlighting the significance of different characteristics of FRP types and the different methods of wrapping. However, it would be preferable to include the schematic design of the beams (e.g., dimensions and reinforcing details) and the configuration of the FRP layers (e.g., numbers and thickness), in addition to providing examples of shear capacity from experimental data, codes, and the algorithm as values for clear comparison and further verification.

On the other hand, in 2016, Chisari and Bedon developed a multi-objective optimization approach to optimize FRP jackets for the strengthening of RC frames, utilizing a multi-objective Genetic Algorithm (GA) optimization, to achieve maximum frame workability and reduce FRP amount/cost. Figure 6 depicts the flow chart of the process. To apply the model, a case study of a three-story, three-bay RC frame was used, as illustrated in Fig. 7. For the aforementioned reinforced concrete frame, an OpenSees (2009) finite element model was established, and after that, GA optimization analyses were performed with six design parameters (two column categories by three different floors), allowing various thicknesses of FRP layers for interior and exterior columns and also for each floor of the frame. These thicknesses could range from 0 (no strengthening) to 2 mm with 0.001 mm incremental increases. Following the establishment of the design parameters' trial values, the reinforced structure's finite element model was developed. The study conducted a pushover analysis for each trial, which produced the following results: maximum steel strain in each reinforced concrete component, inter-story drift for each applied load step, and a capacity curve for the reinforced concrete frame in terms of base shear and top displacement. Two different loading conditions were used for each finite element model, based on the horizontal distribution of loads: a first-mode proportional distribution (D1) and a mass-proportional distribution across the frame height (D2). Figure 8 displays the Pareto fronts for both the D1 and D2 loading conditions that were developed during the study. The findings could be concluded as follows: the optimal FRP thicknesses acquired from the whole optimization study are reported

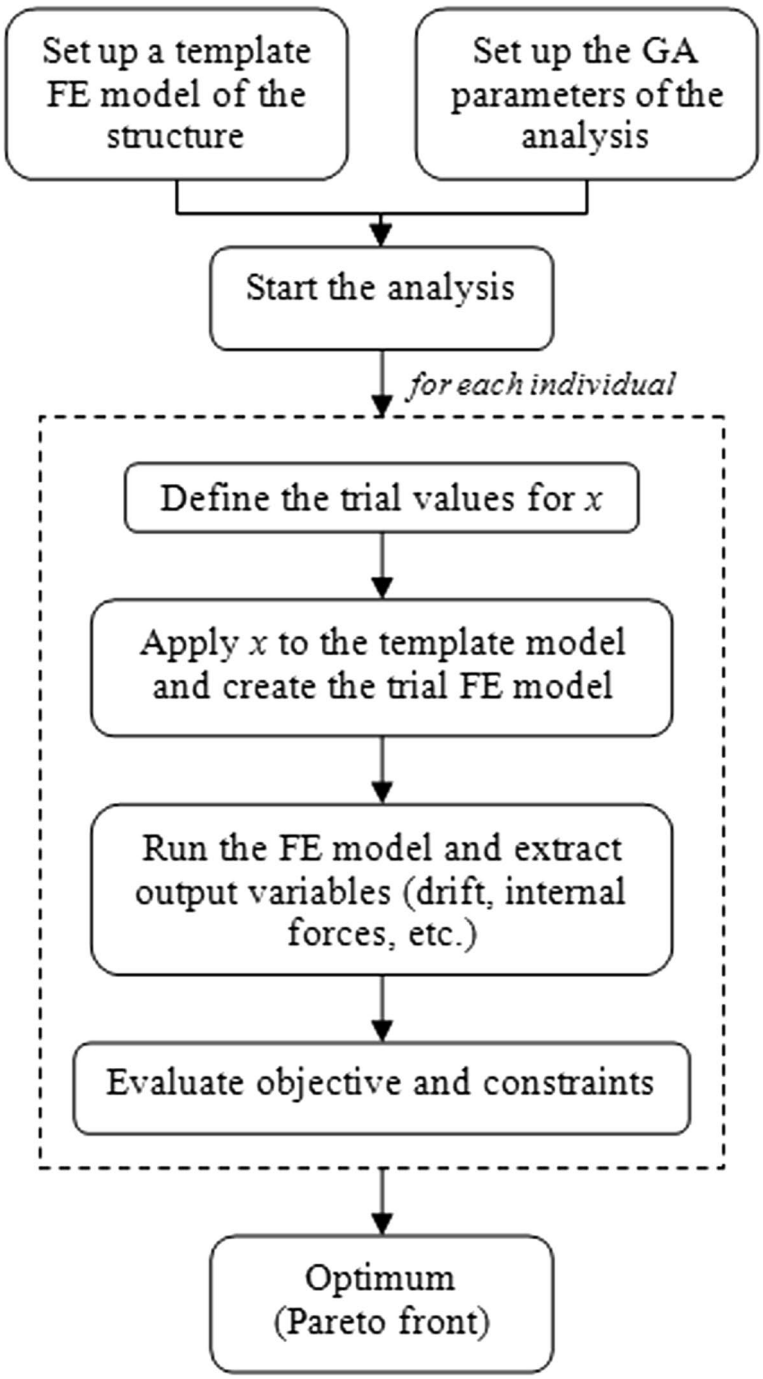

Fig. 6 Flow chart of the optimization process [10]

in Table 9. The biggest impact on the case study's ideal solution came from strengthening the internal columns on the first floor. It is possible to improve the ductility further by increasing the thickness of FRP used in the exterior columns, even after reaching the maximum allowable thickness of FRP for the internal columns (which was 2 mm in this study). The algorithm ensures that the FRP thickness of the exterior columns remains as

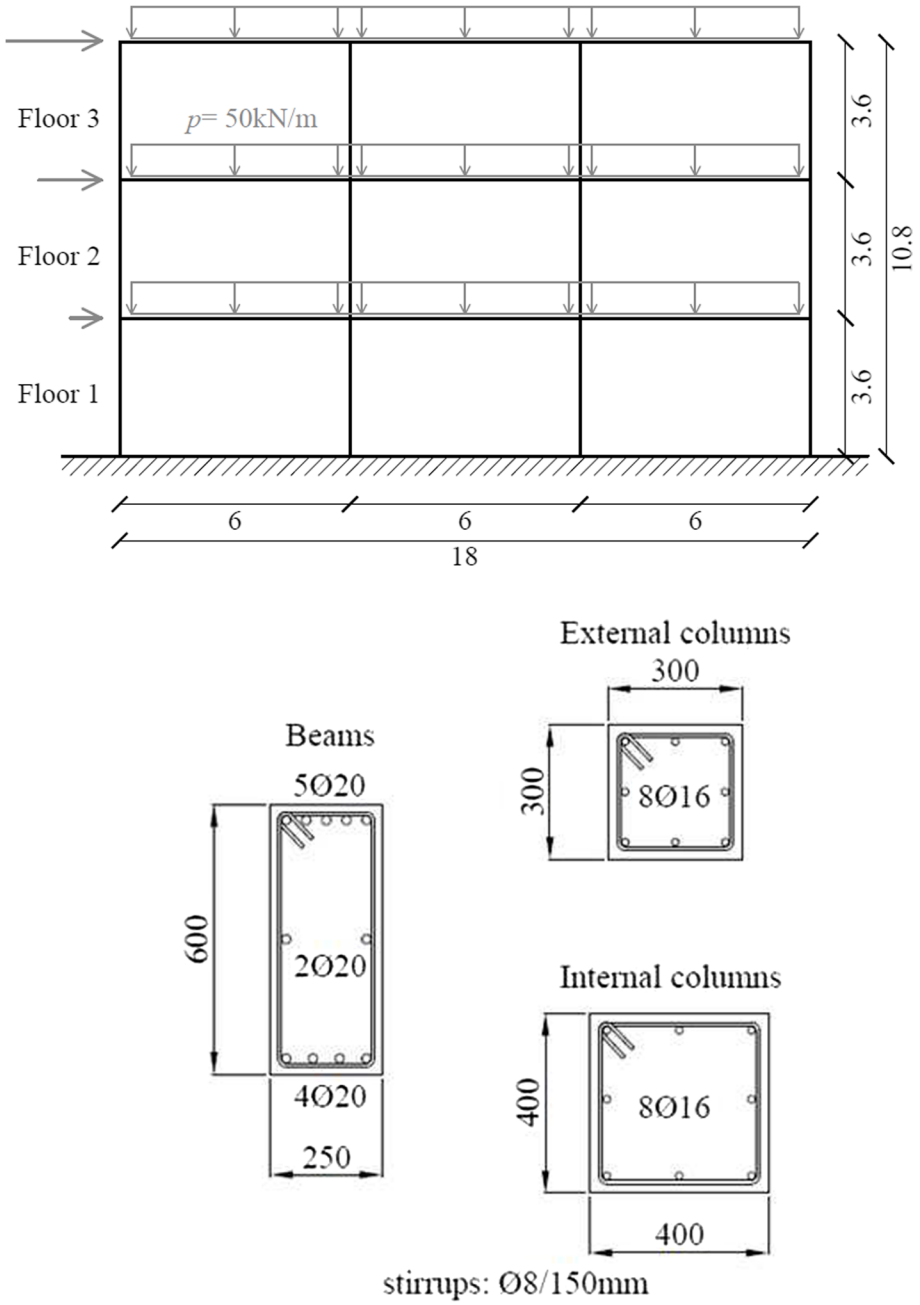

Fig. 7 RC frame geometry, cross section and loads details [10]

minimal as possible while still achieving the desired ductility range. Due to its significant contribution to total cost and relatively insignificant effects on ductility increase, in terms of the structure's overall response, the strengthening on the remaining building floors is notably less significant. As a result, the FRP thickness is carefully controlled, as shown in Fig. 8 and Table 9 [10].

Commenting on the preceding case study, presenting the used frame schematic design details and using two methods for the horizontal load distributions was significant. Additionally, the algorithm's flexibility to use different thicknesses for the internal and

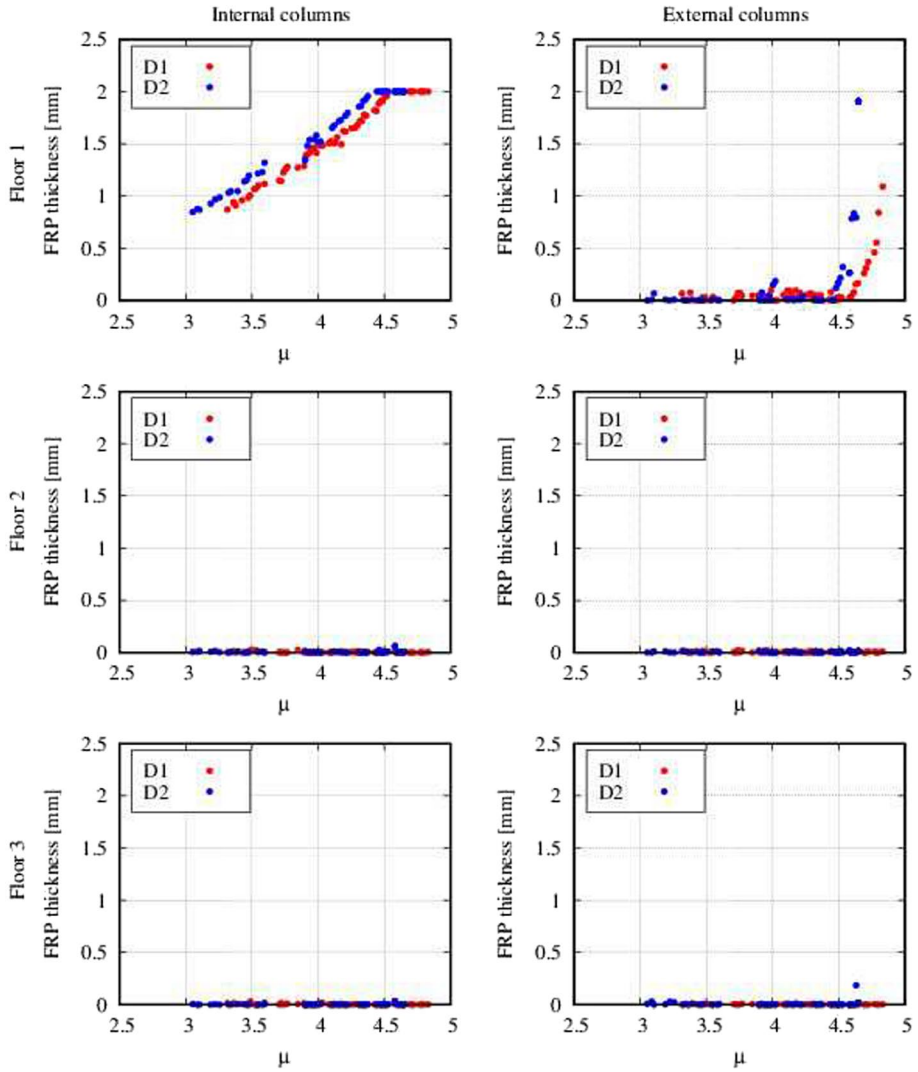

Fig. 8 Pareto front [10]

Table 9 Optimal solutions [10]

Story	Column type	Thickness (mm)			
		Ductility optimal		Cost optimal	
		D1	D2	D1	D2
1	External	1.090	1.906	0.066	0.000
	Internal	2.000	2.000	0.870	0.846
2	External	0.010	0.013	0.016	0.001
	Internal	0.005	0.006	0.000	0.005
3	External	0.002	0.016	0.001	0.008
	Internal	0.001	0.003	0.014	0.005

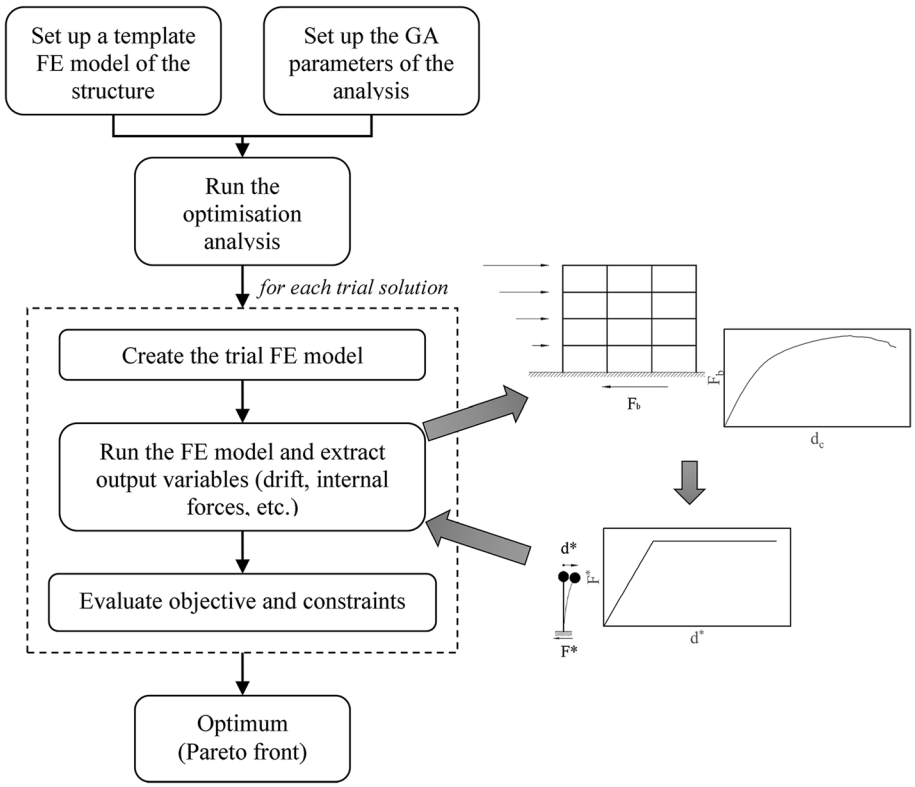

Fig. 9 Process flow diagram for optimization [11]

external columns, considering their floors, was beneficial as it helps to reach the optimal solution. However, it would have been desirable to compare the results with experimental data or manual solutions to verify and prove the algorithm's success. Moreover, due to the symmetrical geometry of the proposed case study, it would be useful to conduct a case study with an asymmetrical model to cover more real-life scenarios.

As an extension of their previous research, in 2017, Chisari and Bedon released a study on the use of a multi-objective Genetic Algorithm (GA) to optimize the configuration of FRP rehabilitation of reinforced concrete frames. The design objective was to generate the most cost-effective and high-performing solution while achieving the damage standards required by workability and ultimate earthquake risk levels for the performance-based design, which has the following performance objectives: operational (O), immediate occupancy (IO), life safety (LS), and collapse prevention (CP) (Fig. 9). A realistic case study, which is part of an office building located in Catania (Italy) and designed without consideration of the seismic action, was conducted and illustrated in Fig. 10. For the purpose of pushover studies, two different load distributions were developed. The first distribution, D1, featured horizontal loads that increased in proportion to the mass matrix and first-mode shape. The second distribution, D2, featured horizontal loads that increased in proportion to the seismic masses. The capacity curve of the original frame, in terms of base shear and top displacement, is shown in Fig. 11. Subsequently, using eight design parameters expressed by the FRP wraps' thicknesses (two column categories by four different floors), an analysis of the GA optimization was undertaken. The FRP thicknesses were permitted

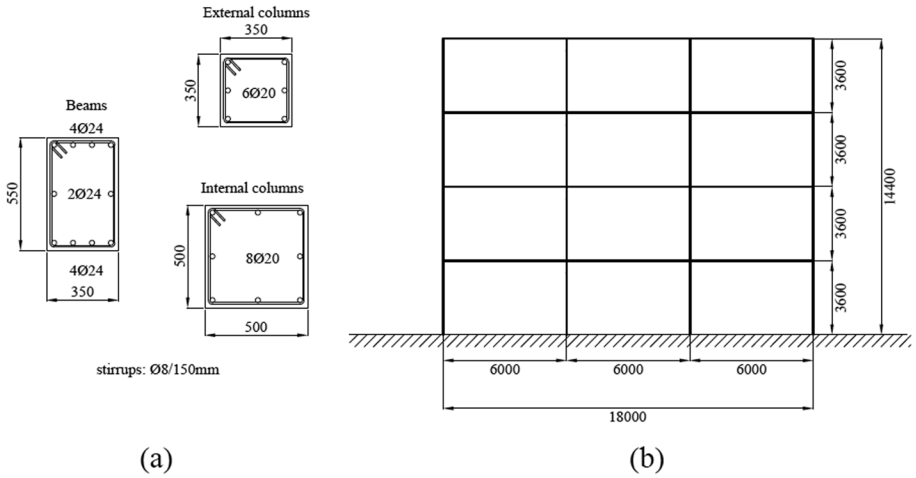

Fig. 10 RC frame geometry and cross section [11]

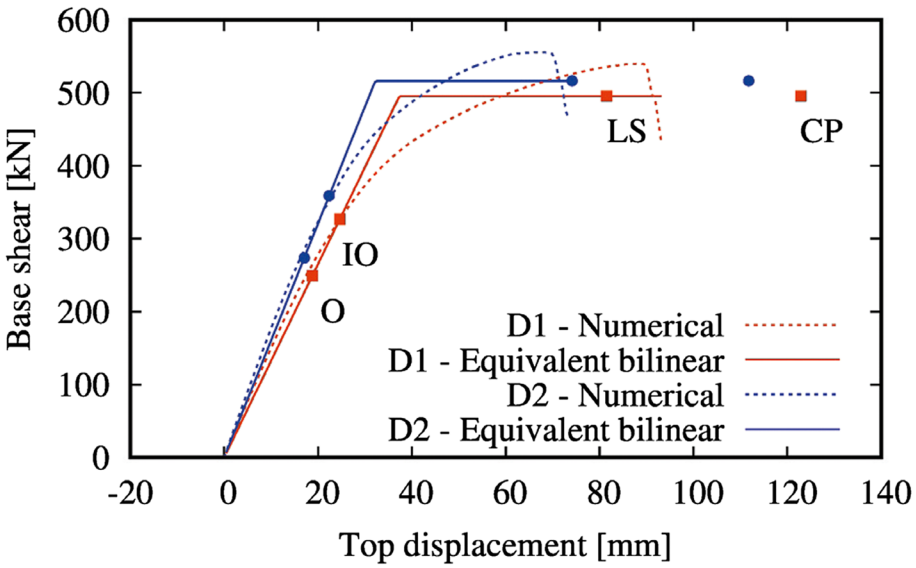

Fig. 11 Capacity curves for bare frame [11]

to range from 0 (no strengthening) to 2 mm, with 0.001 mm increments. Then the pushover analyses were conducted for the GA trials, and the Pareto fronts obtained are shown in Fig. 12. The following is a summary of the findings: The Pareto fronts showed that retrofitting is only feasible on the first floor's internal columns, and FRP wraps were often worthless on the other floors and on external columns (Fig. 13). It is clear from displaying the capacity curves of the optimal solution in relation to the two objectives (cost and ductility) that the strictest constraint (CP top displacement obtained for D2 force distribution) was met without safety margins; in other words, the target was reached at the end of the capacity curve in order to minimize cost. However, the optimal option gives a wider safety margin against collapse according to the ductility target [11].

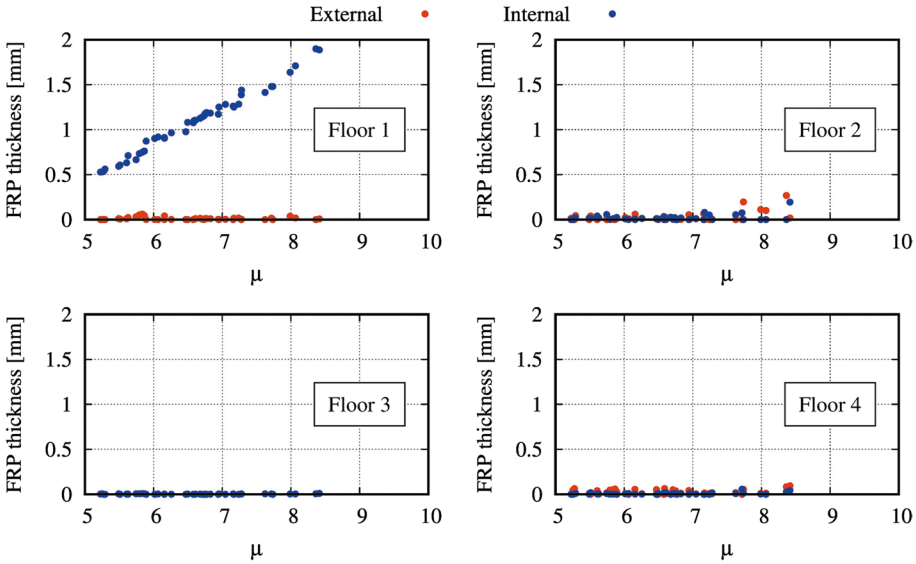

Fig. 12 Pareto front [11]

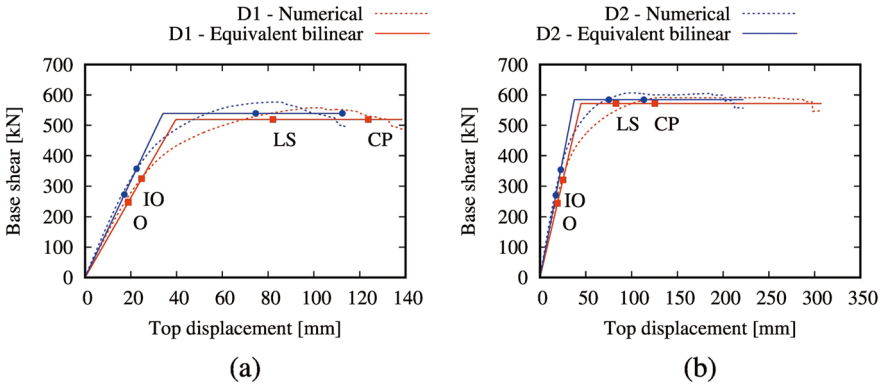

Fig. 13 Curves of retrofitted frame capacity: **a** best cost solution; **b** the best ductility solution [11]

Analyzing the preceding case study, it is significant to demonstrate the capacity curve of the original and retrofitted frames as it highlights how well the FRP works as a strengthening material. It is also important to present the schematic design details of the used frame and use two methods for the horizontal load distributions. The algorithm's flexibility to use different thicknesses for the internal and external columns considering their floors is beneficial as it helps to achieve the optimum solution. However, it would be desirable to compare the results with experimental data or manual solutions for the purpose of verification and proof of the algorithm's success. Additionally, due to the symmetrical geometry of the proposed case study, it would be beneficial to conduct a case study with an unsymmetrical model to cover more scenarios in real life.

Moreover, Baji et al. (2018) [33] utilized a genetic algorithm to present an optimization strategy for determining the required number of layers of FRP for retrofitting reinforced concrete columns with FRP and for determining the time needed for corrosion protection retrofitting. The approach being proposed relied on two methods, namely renewal theory and time-dependent reliability, with the goal of identifying the most

favorable time that would result in the lowest projected number of failures and the ideal number of layers required to achieve this outcome. The comprehensive process includes the initial design, calculation of the pre-strengthening residual strength based on the decrease in steel area, calculation of the post-strengthening residual strength based on the decline in FRP composites' ultimate strength over time, and finally, GA optimization for the degree and time of strengthening. This process can be summarized as follows: inputting the necessary section dimensions, material characteristics, and environmental effects; establishing models for steel and FRP materials' deterioration; determining the nominal loads and capacity of the RC column R_n; setting a starting number for the RC column's post-strengthening capacity αR_n (where α is greater than or equal to 1); giving the time of strengthening, t_r, a starting value within the structure's lifetime, t_l; the strength that remains in the RC column is calculated as a function of time using pre-existing models of deterioration, and this calculation is done for both before and after the process of strengthening; the likelihood of failure is calculated based on time, both prior to and subsequent to reinforcing; the process checks whether the reasonable probability of failure is greater than or equal to the likelihood of failure; if this condition is not met, the process returns to set a new starting number for the strengthening time, t_r; determining how many failures are anticipated for the structure's lifetime; iterating the stages from setting the time of strengthening t_r to computing the predicted the failures' number to find the best value of the time of strengthening t_r that minimizes the overall expected number of failures; increasing the RC column's post-strengthening capacity if convergence fails; and finally, determining the number of layers necessary from FRP based on the desired post-strengthening value. The ACI 440.2R issued in 2008 and ACI 318 issued in 2011 design code principles were used to design the RC column. To demonstrate how the proposed methodology can be used, an example of an RC circular column with a 0.5-m diameter was provided. The specifications of the materials included: for concrete, $f_c' = 25$ MPa, $E_c = 23{,}500$ MPa, $\varepsilon_{c0} = 0.002$, and $\varepsilon_{cu} = 0.003$; for steel, $\rho = 0.03$, $f_y = 414$ MPa, and $E_s = 200$ GPa; for FRP, $t_f = 1.2$ mm, $\sigma_{fu} = 887$ MPa, $E_f = 64{,}900$ MPa, and $K_\varepsilon = 0.55$. The findings can be summarized as follows: Table 10 provides an overview of degradation models based on various corrosion densities for the residual strength of retrofitted RC column sections. To fulfill the restrictions, the post-strengthening strength for the scenario with a corrosion density of $i_{corr} = 3$ μA/cm^2 should be 1.20 times the original strength. According to Fig. 14, the year 51 corresponds to the minimal predicted number of failures, and the time interval [43, 56] was the viable response area where both optimization criteria were met. As seen in Fig. 15, the RC

Table 10 Deterioration models [33]

Number of FRP layers	i_{corr}(mA/cm^2)			
	1.0	2.0	3.0	4.0
0	1.15-0.0011t	1.15-0.0020t	1.15-0.0025t	1.15-0.0030t
1	1.46-0.0015t	1.45-0.0025t	1.46-0.0035t	1.45-0.0040t
2	1.58-0.0017t	1.58-0.0028t	1.58-0.0037t	1.58-0.0045t
3	1.70-0.0018t	1.69-0.0029t	1.70-0.0039t	1.69-0.0046t
4	1.80-0.0018t	1.78-0.0030t	1.78-0.0040t	1.78-0.0050t
5	1.90-0.0018t	1.88-0.0031t	1.90-0.0042t	1.88-0.0051t

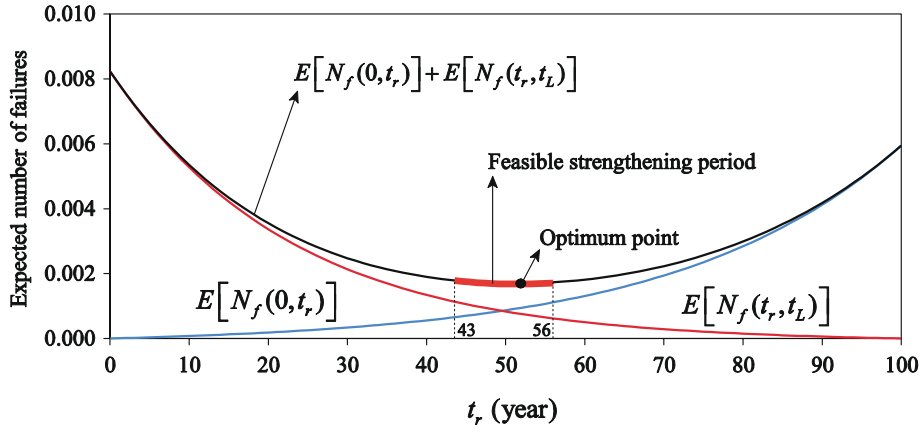

Fig. 14 Optimum time at $i_{corr} = 3\mu A/cm^2$ [33]

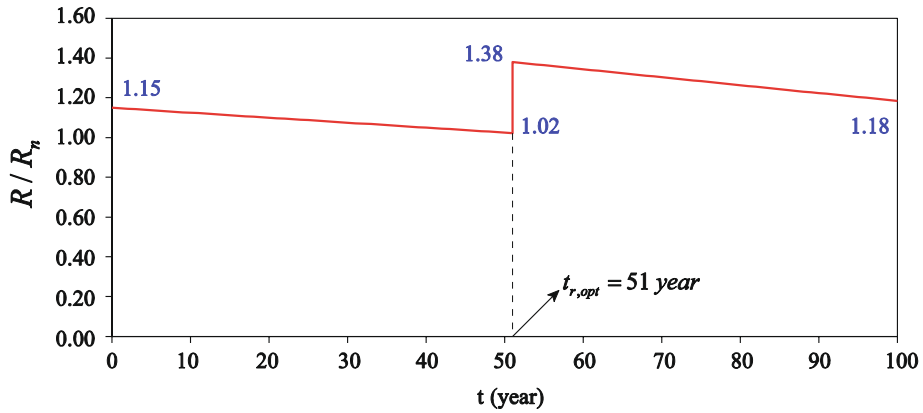

Fig. 15 Residual strength prior to and following the ideal time at $i_{corr} = 3\mu A/cm^2$ [33]

column residual strength under consideration drops to 0.89 of its initial strength (i.e., 1.15 R_n) after 51 years. The residual strength then rises to 1.20 of the original strength when two layers of FRP composites were applied, and as shown in Fig. 16, the residual strength after 51 years when utilizing two layers of FRP wrap was 1.38 R_n. Finally, the best strengthening strategy was to add two layers of FRP confinement to the RC column 51 years after the time of the original design. Table 11 displays the impact of various corrosion rates on the strengthening strategy. As can be observed, increasing the corrosion rate necessitates adding additional FRP layers early [33].

Discussing the prior case study, the approach follows logical phases to demonstrate the progression of the column's condition from the initial case to the degraded case, then to the reinforced condition, and finally to the degradation of it until the end of its useful life. Presenting an example to demonstrate the schematic design details for the used column was significant. Furthermore, it was beneficial to demonstrate the strength of the original and retrofitted columns since it highlighted how well the FRP worked as a strengthening material. However, it would be desirable to compare the results with experimental data or manual solutions for the purpose of verification and proof of the algorithm's success.

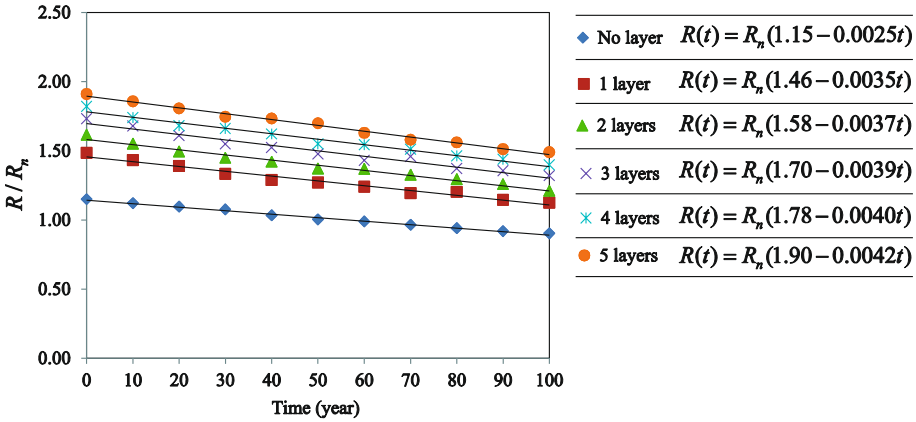

Fig. 16 Normalized residual strength for various numbers of FRP layers at $i_{corr} = 3\mu A/cm^2$ [33]

Table 11 Effect of corrosion rate [33]

$i_{corr}(mA/cm^2)$	$t_{r,opt}$(year)	Number of FRP layers	$R(t_{r,opt})/R_n$
2	68	1	1.27
3	51	2	1.38
4	43	3	1.44

Furthermore, in 2021, a methodology employed by Ebid and Deifalla involved genetic programming to create a formula that predicts the shear strength of FRP reinforced beams, in the presence or absence of stirrups. They gathered a collection of 553 test samples, where 425 tests were conducted on beams lacking stirrups, and 128 tests were conducted on beams containing stirrups. The collection of data was partitioned into two sections: a learning set comprising 363 samples from 59 studies and a verification set comprising 190 samples from 19 studies. The test data was obtained for rectangular beams with reinforcement bars and with or without stirrups, including varying percentages of AFRP, GFRP, and CFRP. The schematic design of the beams in the training set ranged from 73 mm to 938 mm in depth, 89 mm to 1830 mm in width, 0.09 to 4.00% for the longitudinal reinforcement ratio, 0.00 to 1.50% for the shear reinforcement ratio, and 1.50 to 16.2% for the effective span-to-beam depth ratio. The validation set schematic design ranged from 150 mm to 883 mm in depth, 120 mm to 1000 mm in width, 0.12 to 4.00% for the longitudinal reinforcement ratio, 0.00 to 0.89% for the shear reinforcement ratio, and 1.50 to 5.2% for the effective span-to-beam depth ratio. The research program consisted of four trials, starting with a minimal degree of complexity (just two levels) and gradually increasing to a higher degree of complexity (five levels). The trials were carried out repeatedly until the minimum sum of squared errors (SSE) was attained, which indicated the most precise formula for the given difficulty level, and this is presented in Table 12. The efficiency of the suggested formula was evaluated by comparing its SSE and coefficient of determination R^2 with those obtained through testing and using techniques described in existing literature, which are summarized in Table 13. It is possible to deduce the following conclusions: The precision levels of the Nehdi et al. (2007) [17]

Table 12 Brief of outcomes for trials of GA [8]

Trial No.	No. of levels	Proposed Formula	SSE			R^2		
			Tr.	Val.	Total	Tr.	Val.	Total
1	2	Eq. (1)	774,204	584,078	1,358,283	0.710	0.380	0.620
2	3	Eq. (2)	560,215	291,889	852,103	0.796	0.712	0.769
3	4	Eq. (3)	201,246	95,123	296,370	0.922	0.899	0.908
4	5	Eq. (4)	199,417	87,614	287,031	0.926	0.902	0.911

Table 13 Brief of outcomes for GA proposed and other formulas [8]

Formula	SSE	R^2	Slope of best fitting line
ACI 440.1R-15	1,422,937	0.748	0.632
CSA S806-12	606,280	0.841	0.792
Nehdi et al. (2007)	559,155	0.843	0.810
Eq. (4)	287,031	0.911	0.982

model and CSA S806-12 are about equal and fall between equations (2) and (3), while the ACI 440.1R-15 equation was less precise, as it was almost as accurate as equation (2). As the complexity stages increase, the rate of precision improvement decreases, so it would not be worth using more than five-level formulas. As shown in Table 13, the proposed formula (Eq. (4)) provides more reliable estimates than literature models and codes [8].

Reviewing the preceding case study, presenting the schematic design details of the used beams was significant. It was also beneficial to examine the algorithm until it reached the most accurate formula and compared the results with those of other codes and models. The algorithm's training with experimental data from the literature also proved the viability of the suggested model. A series of tests used to verify its results brought them closer to reality and made them more meaningful.

Recently, in 2023, Abathar Al-Hamrani et al. put forward a genetic algorithm-based design equation for estimating the shear strength of one-way slabs composed of basalt fiber reinforced concrete (BFRC) and reinforced with basalt fiber reinforced polymer (BFRP) bars. A model using ABAQUS software was designed in 3D and compared to experimental data to investigate how certain factors—such as the longitudinal reinforcement ratio, effective depth, concrete compressive strength, shear span-to-depth ratio, and the volume of basalt microfibers—affect the shear strength of BFRC-BFRP slabs. The design parameters were subjected to a sensitivity analysis using the same model. Ultimately, a design equation was proposed based on a genetic algorithm. In order to test the efficiency of the suggested model, a collection of 49 one-way slabs that had been tested for shear was gathered from various sources. The ACI 440.1R-15, CSAS806-12, JSCE-97, and ISIS 2007 design codes and standards were used to assess the effectiveness of the suggested model. The results indicated that the suggested model performed better than the known design codes and guidelines, with a coefficient of variation (COV) of 17.91% and a mean ratio of anticipated to experimental shear capacity (V_{pred}/V_{exp}) of 0.97. In contrast, the ACI 440.1R-15, ISIS 2007, and JSCE-97 design codes produced

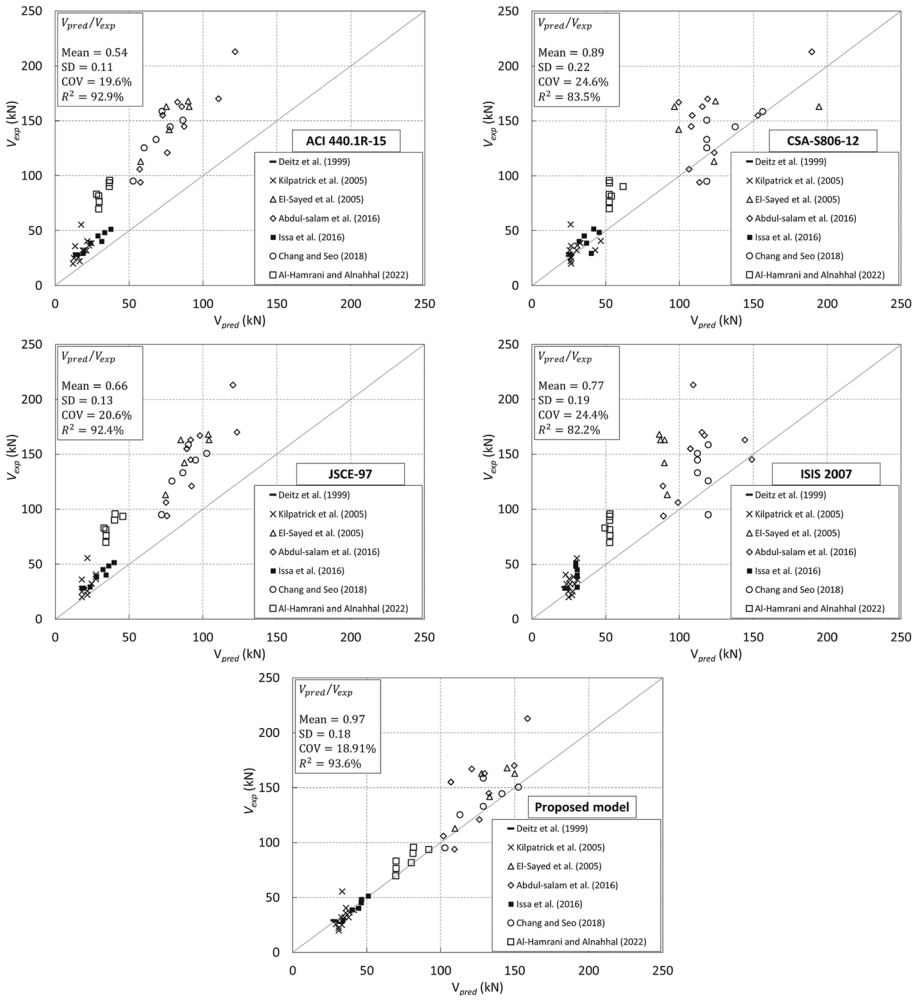

Fig. 17 Experimental shear capacity versus anticipated based on the experimental database [20]

overly conservative predictions, with average $V_{\text{pred}}/V_{\text{exp}}$ values of 0.54 ± 0.11, 0.66 ± 0.13, and 0.77 ± 0.19, respectively, and COVs of 19.6%, 20.6%, and 24.4%. The CSA-S806-12 design code produced fewer conservative predictions, with an average $V_{\text{pred}}/V_{\text{exp}}$ of 0.89 ± 0.22 and a COV of 24.6%, as shown in Fig. 17. The ratio of longitudinal reinforcement, effective depth, and compressive strength had the greatest impact on shear capacity, with proportional contributions of 42.58%, 24.58%, and 10.30%, respectively. This finding was consistent with current FRP-RC standards and design recommendations, particularly ACI 440.1R-15, CSA-S806-12, ISIS-2007, and JSCE-1997. The inclusion of BMF was also deemed significant statistically, with a percentage contribution of 7.26%. As stated in the literature, this could indicate an increased shear capacity of BFRC specimens resulting from the BMF bridging the diagonal shear fracture, reinforcing the damaged surface [20].

In discussing the prior case study, it was significant to verify the suggested model using experimental data from the literature. This step made the results more reliable. Additionally, comparing the results with widely used codes and standards helped clarify the algorithm's efficiency in generating better and more realistic results. Nonetheless, it

would have been preferable to expand the database to minimize biases. Also, it would have been better to gather the database from the literature with a greater emphasis on BFRP type rather than two types of FRP. This is because the major goal of the research was to forecast the shear capacity for BFRC-BFRP slabs.

Particle swarm optimization (PSO) to optimize FRP

In this subsection, case studies from literature are presented to discuss the particle swarm optimization (PSO) algorithms used to optimize fiber-reinforced polymer (FRP) utilization in designing or retrofitting reinforced concrete (RC) structures in flexure and structural health monitoring. A research was conducted by INNOCENTE et al. in 2007 for minimizing the cost of a concrete beam reinforced with FRP against flexural force using the PSO algorithm while satisfying the design codes (ACI 440.1 R-06). Two optimizers were proposed, and the key differences between them were in the technique they utilized (one used the feasibility technique, while the other used the penalization method) and in the way they computed the reinforcement (deterministic at each time step while the other was treated as another object variable to be optimized). A few examples of how the approach was incorporated in the two proposed optimizers have been embedded in both of them. The goal was to demonstrate their applicability and effectiveness in dealing with an overly simplified optimal design problem. The algorithms were used to determine the best cost-effective design of a pin-jointed concrete beam reinforced with glass fiber-reinforced polymer (GFRP) with a consistent load. Three sets of costs were studied, including the costs of materials, transportation, and formwork as shown in Table 14. The beam had a width from 20 cm to 100 cm, a height from 20 cm to 200 cm, and a span of 5 m. The following conclusions can be reached from the findings: optimal designs are indicated in Tables 15 and 16, for both the height limited to 200 cm and 35 cm, respectively. It is worth noting that the first optimizer's output for height limited to 35 cm required considerable resources due to the deterministic reinforcement calculation, while the major downside of the penalization strategy used in the second optimizer was that it required problem-specific adjustment of the penalization coefficients, with too high penalizations leading to suboptimal solutions and too low

Table 14 Sets of costs for materials [18]

			CASE A	CASE B	CASE C	
Concrete			**100**	**100**	**100**	
Shuttering			**25**	**2.95**	**35**	
Size	**Diameter φ_b(mm)**	**f'_{fu}(MPa)**				
#2	6.35	825	0.498361392	0.58630752	0.274098766	COSTS
#3	9.53	760	1.099572057	0.514049937	0.76970044	
#4	12.70	690	1.543445568	1.815818315	0.848895062	
#5	15.88	655	2.328630417	2.739565196	1.280746729	
#6	19.05	620	3.285252527	3.285252527	1.80688889	
#7	22.23	586	4.419347369	5.199232198	2.430641053	
#8	25.40	550	5.72378227	6.733861494	3.148080249	
#9	28.65	517	7.241397324	8.519290969	3.982768528	

Table 15 Optimal designs obtained by the two proposed optimizers, where the height is restricted to a maximum of 200 cm [18]

CASE	b (m)	h (m)	n x φ_b	COST			
				Concrete	Shuttering	Reinforcement	TOTAL
FIRST OPTIMIZER							
A	0.2124	0.5346	3 x #6	11.3547	32.0395	9.8558	53.2499
B	0.2124	0.5346	3 x #6	11.3547	3.7807	11.5950	26.7304
C	0.2401	0.4883	3 x #7	11.7227	42.5823	7.2919	61.5970
SECOND OPTIMIZER							
A	0.2124	0.5346	3 x #6	11.3543	32.0387	9.8558	53.2488
B	0.2124	0.5346	3 x #6	11.3546	3.7806	11.5950	26.7302
C	0.2401	0.4882	3 x #7	11.7217	42.5792	7.2919	61.5928

Table 16 Optimal designs obtained by the two proposed optimizers, where the height is restricted to a maximum of 35 cm [18]

CASE	b (m)	h (m)	n x φ_b	COST			
				Concrete	Shuttering	Reinforcement	TOTAL
FIRST OPTIMIZER							
A	0.5067	0.3482	9 x #6	17.6414	30.0756	29.5673	77.2843
B	0.8801	0.3447	21 x #3	30.3362	4.6300	10.7950	45.7612
C	0.5067	0.3482	9 x #6	17.6414	42.1059	16.2620	76.0093
SECOND OPTIMIZER							
A	0.5067	0.3500	7 x #7	17.7354	30.1682	30.9354	78.8390
B	0.5067	0.3500	9 x #6	17.7341	3.5597	29.5673	50.8611
C	0.4776	0.3500	6 x #8	16.7174	41.2174	18.8885	76.8233

penalizations leading to infeasible solutions. The second optimizer, which computes the reinforcement as a design variable, seems to be a step closer to an optimizer capable of handling more complex optimal designs. Another benefit of taking this into account was how much simpler it was to add, remove, or modify constraints. One example would be to incorporate the shear design [18].

Discussing the prior case study, it was beneficial to compute the results from two optimizers using different concepts and compare them. However, it would have been preferable to present the manual findings discussed in the paper for verification purposes. This would have demonstrated how important it is to apply these optimizers and gauge the effectiveness of the method. Additionally, it would have been desirable to clarify the basis of the three sets of costs that were studied.

Furthermore, in the context of structural health monitoring, Perera et al. (2014) [34] offered a multi-objective particle swarm optimization approach as a model used to minimize the difference (error) between the real response from experimental tests and the response predicted by computational software models based on strain measurements under monitored loading to identify debonding damage of RC beams retrofitted with FRP. Implementing such a proposal appears to be crucial in preventing unexpected and fragile failure modes of FRP bond from transitional parts of FRP-strengthened structures. The variations between the recorded strains of the damaged and undamaged structures

were used to develop objective functions. Simplified spectral numerical models based on Fourier polynomials, Figs. 18 and 19, 2D finite element models, Fig. 20, and experimental studies, Figs. 21 and 22, were conducted for beams before and after debonding damage with various loading configurations and damage scenarios. The damage existence probability (PDE) was determined using the statistical distributions of the damage indices. Estimating the possibility of the damage index at a certain degree of confidence was its basic idea. The PDE was scaled from 0 to 1, where values near 0 suggest that it was extremely

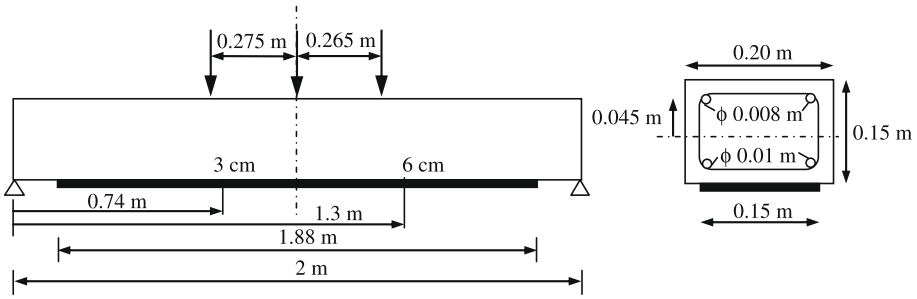

Fig. 18 Numerical study scheme [34]

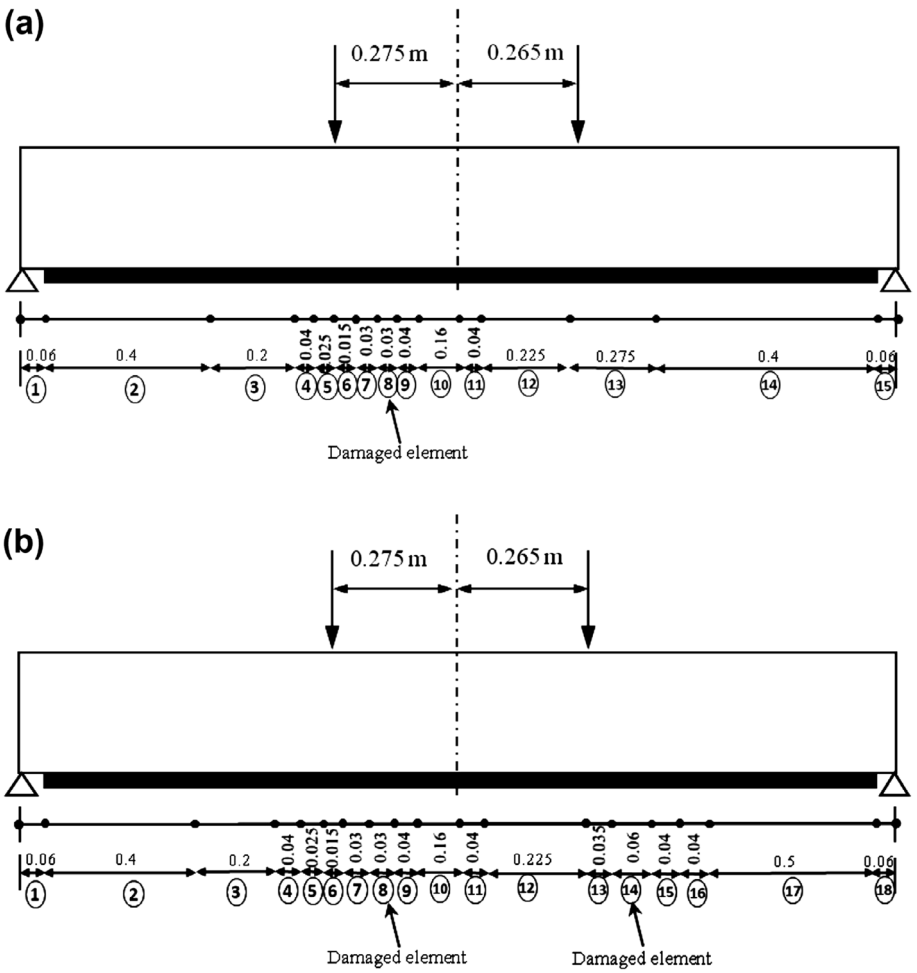

Fig. 19 Spectral element meshes. **a** A scenario with a single damage. **b** A scenario with multiple damages [34]

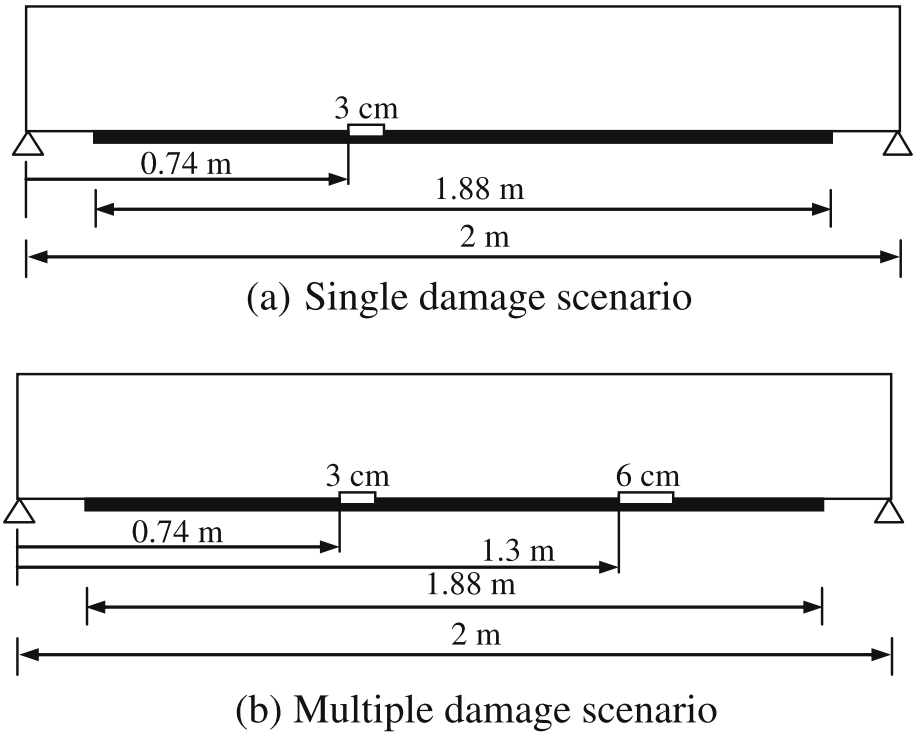

Fig. 20 **a** A scenario with a single damage. **b** A scenario with multiple damages [34]

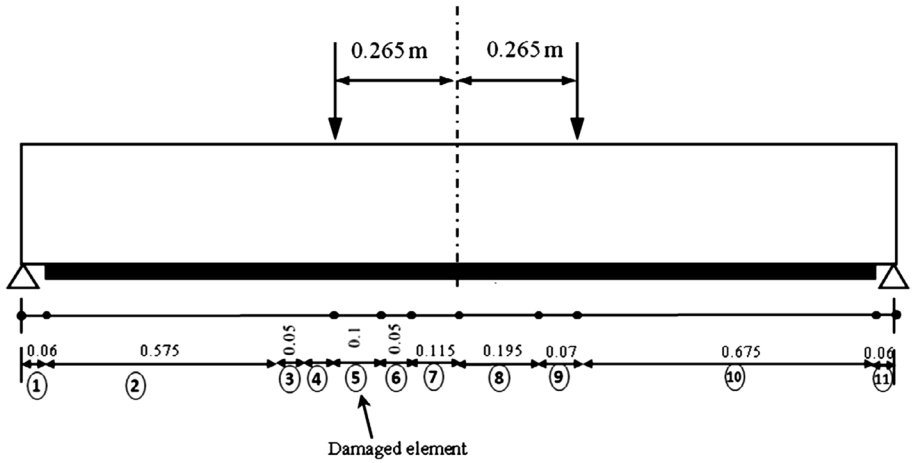

Fig. 21 Experimental beams spectral element mesh [34]

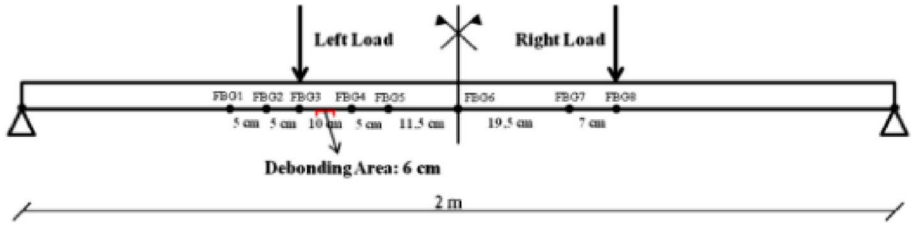

Fig. 22 Experimental beams test configuration [34]

unlikely to deteriorate, and values close to 1 imply that the element would most likely deteriorate. The following is a summary of the findings: Figs. 23 and 24 demonstrate the correlation between an experimental study of FRP strain profiles acquired for the control beam and a simplified spectral numerical model; only the data correlating to the positions of the sensors were displayed. The damage indices for each element of the multi-objective algorithm are displayed in Fig. 25, where the damaged region may be recognized by the fact that the highest values were near the debonded zone (element 5). The PDE is computed for each element and is presented in Fig. 26. Damaged elements (element 5) have large probabilities, whereas those that are undamaged have probabilities that are much lower than 1. The suggested approach seems to have high potential as a non-destructive assessment method when paired with Fiber Bragg grating (FBG) sensors, which have high resolution and accuracy for locally detecting strain [34].

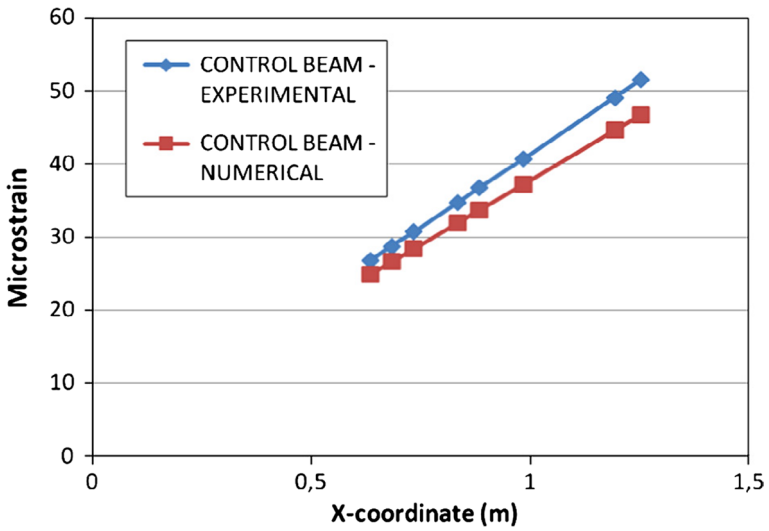

Fig. 23 Distribution of FRP strain under a focused load placed to the right of the midspan. Original beam [34]

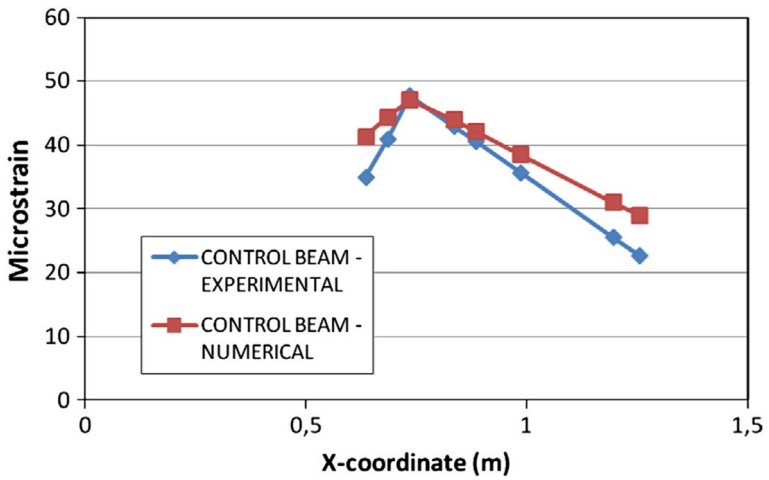

Fig. 24 Distribution of FRP strain under a focused load placed to the left of the midspan. Original beam [34]

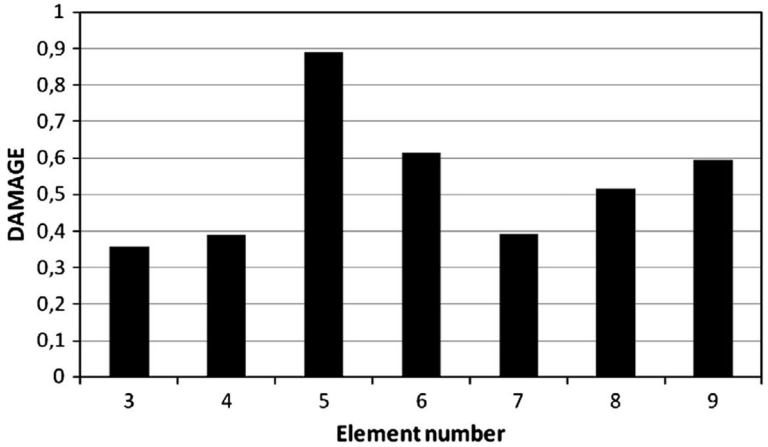

Fig. 25 Calculated damage distribution by the algorithm [34]

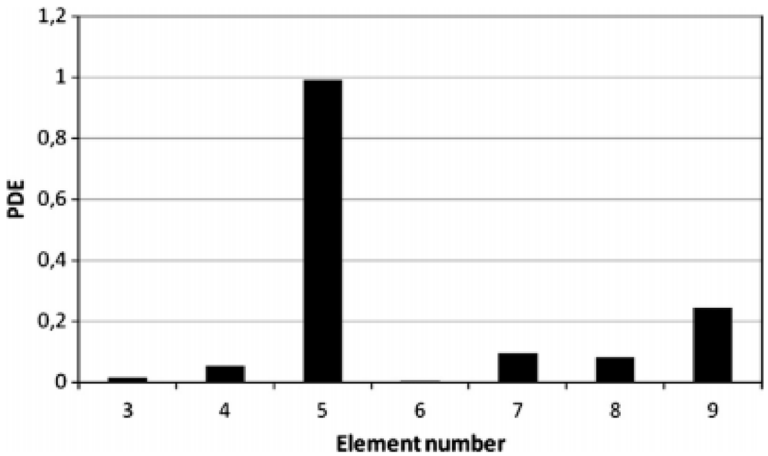

Fig. 26 Probability of damage existence [34]

Regarding the previous case study, creating an automated methodology for using FBG sensors was found to be beneficial. These sensors can monitor strain with high resolution and precision in specific regions, enabling the objective function to achieve its aim and the automated model to produce realistic results in an unsupervised mode. However, it was desirable to demonstrate the correlation between a simplified spectral numerical model and experimental studies of FRP strain profiles for the damaged beams after debonding.

Particle swarm optimization (PSO) and Genetic algorithm (GA) in optimizing FRP

In this subsection, a case study from the literature is presented to discuss the use of both genetic algorithms and particle swarm optimization algorithms to optimize the use of fiber-reinforced polymer (FRP) in retrofitting reinforced concrete (RC) structures for seismic purposes. In 2019, Mahdavi et al. proposed two techniques, genetic algorithm (GA) and particle swarm optimization (PSO), for optimizing FRP jacketing for RC frame seismic retrofit, as shown in Fig. 27. The proposed model ensures that all columns have the same amount of plastic hinge rotation capacity while minimizing the amount of FRP material used and maximizing performance by wrapping different

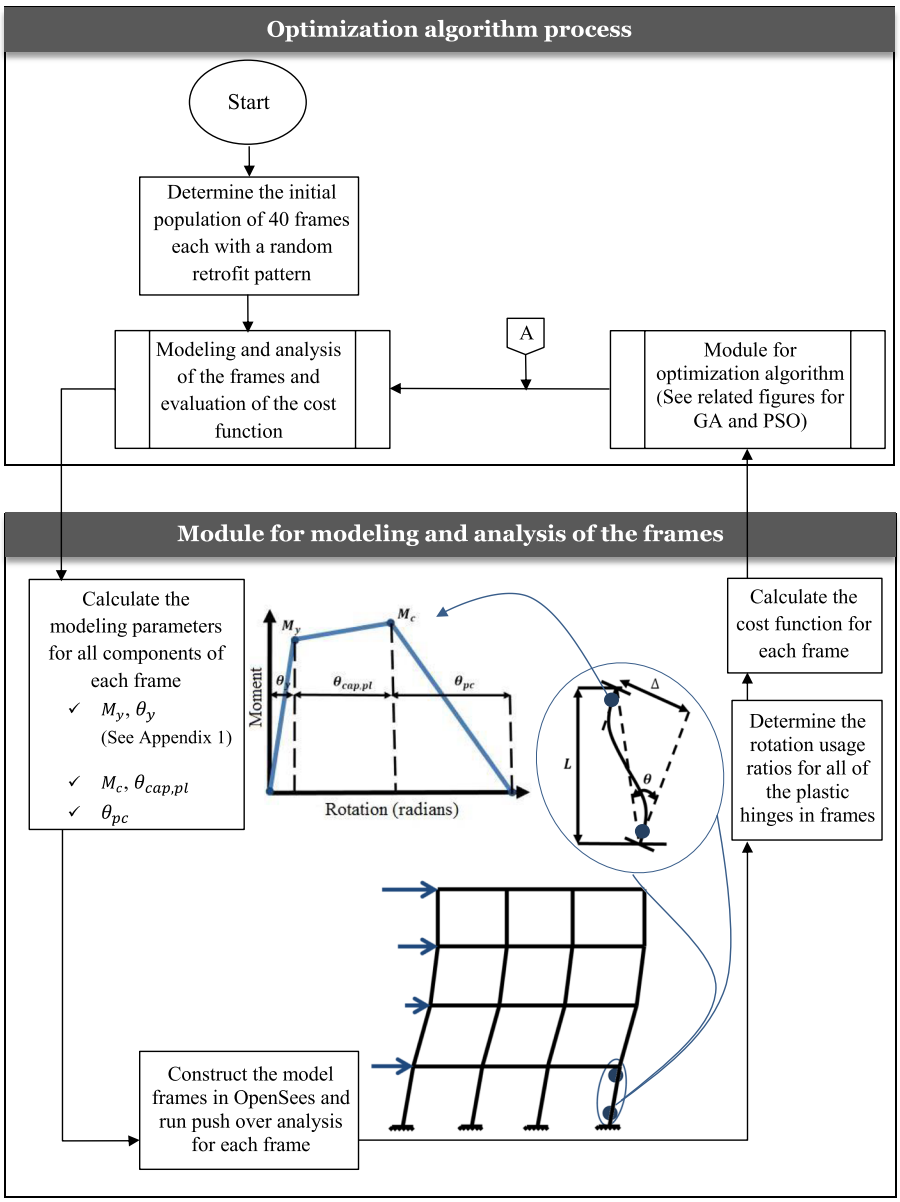

Fig. 27 The flow chart of the optimization process's main module [12]

amounts of FRP wraps around the columns' plastic hinges. A non-ductile, low-rise RC frame shown in Fig. 28 was used as a practical example to evaluate the suggested framework. The RC frame consisted of columns with cross-sections of 500 mm × 500 mm and reinforcement ratios ranging from 0.012 to 0.026 for longitudinal reinforcement and 0.0015 to 0.0039 for transverse reinforcement, in addition to beams with cross-sections of 500 mm × 500 mm and 500 mm × 650 mm and reinforcement ratios ranging from 0.0065 to 0.0125 for longitudinal top reinforcement, 0.0135 to 0.0205 for longitudinal bottom reinforcement, and 0.0028 to 0.0055 for transverse reinforcement. The design variables were considered to be the number of FRP layers. Nonlinear pushover studies were employed to evaluate the capacity of the plastic hinge rotation for FRP-strengthened columns at the life safety level of performance. Both algorithms identified the best

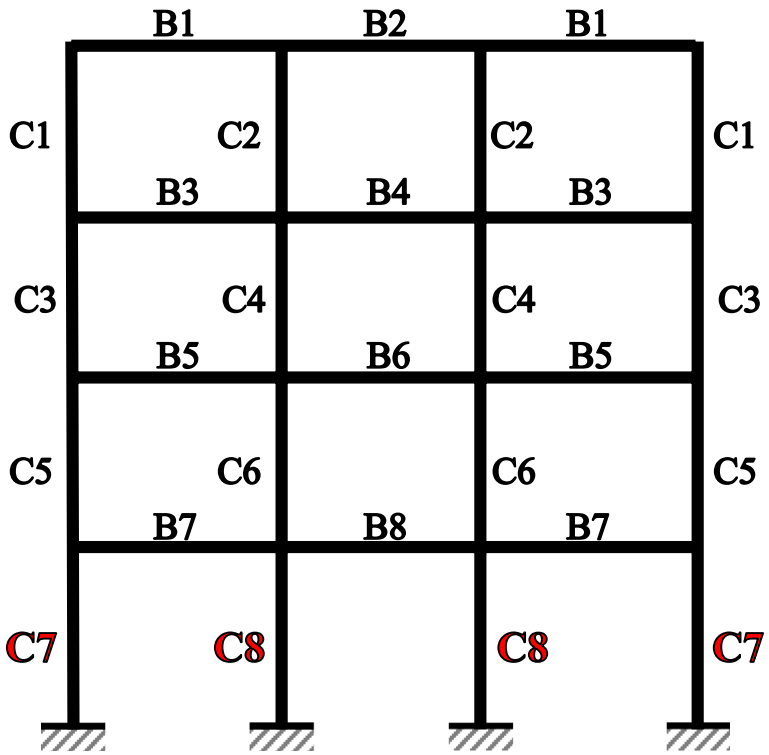

Fig. 28 An example of the case study frame [12]

retrofit strategy for the frame, and for validation purposes, inter-story drift ratios, the capacity curve, and fragility functions were calculated and evaluated against other rehabilitation strategies that had a fixed number of layers for each column. The following is a summary of the findings: the GA arrived at the ideal solution after 832 iterations but had significant oscillations, whereas the PSO converged after 1000 iterations but had less dispersion. Nevertheless, the ideal solution for the case study was the same in both cases, which was for the first floor, six FRP wrapping layers were required for the internal columns and three FRP wrapping layers were required for the exterior columns. Compared to the non-strengthened frame, the maximum roof displacement that the strengthened frame achieved was considerably enhanced, and as shown in Fig. 29, the maximum base

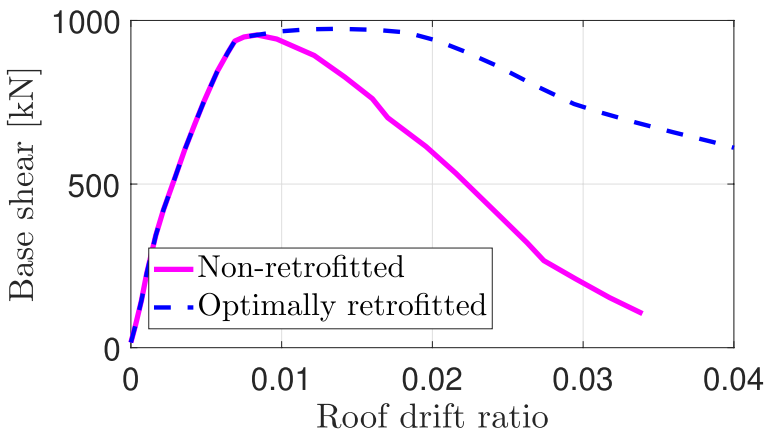

Fig. 29 Pushover curves comparison [12]

shear was greater. Figure 30a shows that after the frame was strengthened, R_i on the first floor was drastically reduced to a value far below unity, which was the desired result. On the contrary, the non-strengthened frame had a value much higher than unity and did not meet the life safety level of performance. As presented in Fig. 30b, the strengthened frame had an inter-story drift ratio of approximately 1.8%, which was lower than the limit of the life safety level of performance as per ATC-40 (e.g., 2%), compared to the original frame's maximum inter-story drift ratio of 2.3% for the first floor (i.e., exceeded 2%). According to Fig. 31, the irregular FRP strengthening scheme acquired from the meta-heuristic algorithm was the best scheme according to all fragility curves for the non-retrofitted frame and retrofit schemes with uniform FRP retrofit plans (for example, the value $n=4$ denotes that all of the first floor's columns are wrapped with four layers of FRP sheets where their plastic hinges were located) [12].

Remarking on the preceding case study, it was beneficial to use two powerful algorithms (genetic algorithm and particle swarm) to obtain the optimal solution. Furthermore, using a case study to compare the results of retrofitted and non-retrofitted frames was significant as it highlighted the importance of FRP. Moreover, the comparison of fragility analyses between the optimal solution retrofit plan and the uniform retrofit plan was beneficial for validation purposes as it presented the significance of the algorithms, especially in using a different number of layers for external and internal columns, which

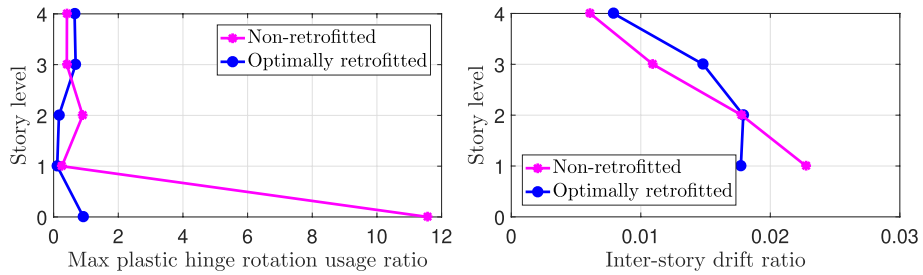

(**a**) Maximum plastic hinge rotation usage ratios (**b**) Maximum inter-story drift ratios

Fig. 30 Structural response comparison. **a** Max. plastic hinge rotation usage ratios; **b** Max. inter-story drift ratios [12]

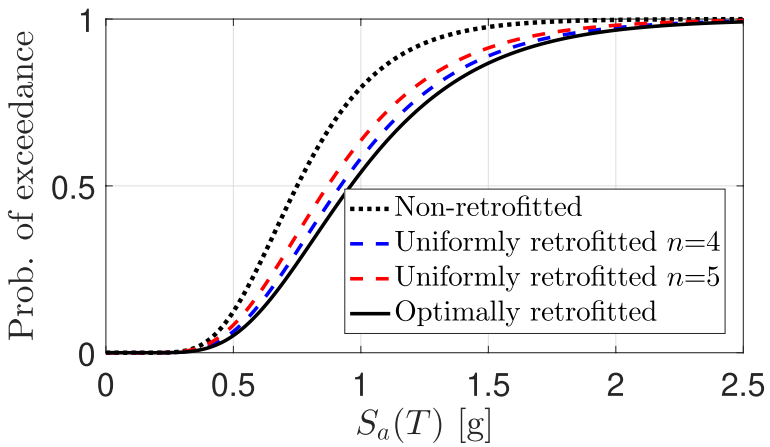

Fig. 31 Fragility curves comparison for the frame [12]

is more practical. However, it would have been desirable to compare the results with experimental data for further verification of the algorithm's success. Moreover, due to the symmetrical geometry of the proposed case study, it would be desirable to conduct a case study with an unsymmetrical model to cover more scenarios in real life.

Generalized regression neural network (GRNN) in optimization of FRP

In this subsection, a case study from the literature is presented to discuss using generalized regression neural network (GRNN) machine learning to optimize FRP materials utilized in designing RC structures in shear. Alam and Gazder (2019) [19] optimized the shear resistance of FRP-reinforced one-way slabs and concrete beams using a GRNN model, as illustrated in Fig. 32. The GRNN model was trained and evaluated using a database consisting of 196 test specimens, of which 148 were used for training and 48 were used for testing. There was no transverse reinforcing in the FRP-reinforced concrete elements. Comparative studies were conducted with the experimental data, as well as commonly used codes and standards, as mentioned in Table 17 and Fig. 33. The mean (μ), standard deviation (STDV), coefficient of variation (COV) for V_{exp}/V_{cal}, and coefficient of determination (R^2) were the statistical parameters used for comparison. The following conclusions can be reached from the findings: In Table 17 and Fig. 33,

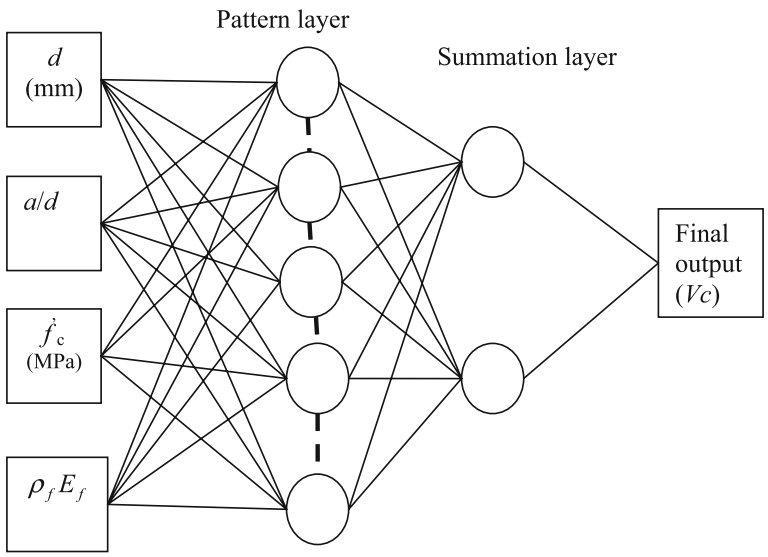

Fig. 32 The general structure of GRNN [19]

Table 17 Test against the expected shear strengths [19]

	Mean (μ)	STDV (σ)	CoV (%)
CSA	1.06	0.32	31
ACI	2.25	1.26	56
JSCE	1.63	0.92	56
BISE	1.37	0.80	58
GRNN (training)	1.02	0.24	23
GRNN (testing)	1.07	0.38	36

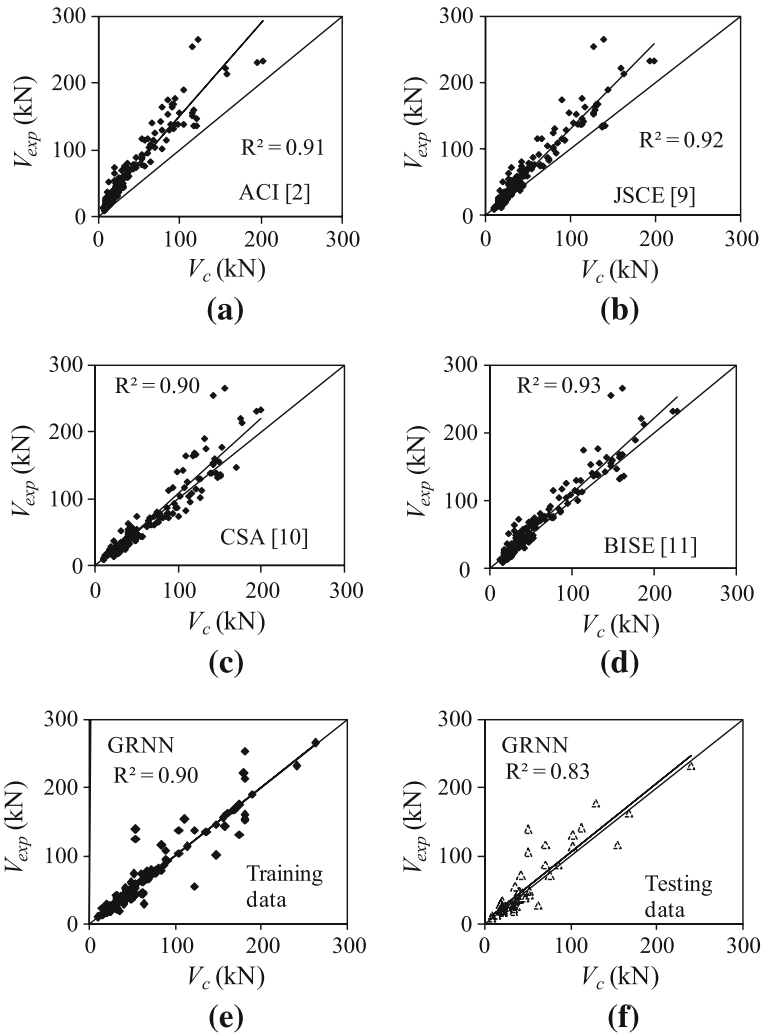

Fig. 33 Experimental vs. estimated shear capacities: **a** ACI; **b** JSCE; **c** CSA; **d** BISE; **e** GRNN training; and **f** GRNN testing dataset [19]

the GRNN model displayed analytically and graphically a more precise estimation than the other four theories. As presented in Table 17, the ACI, JSCE, and BISE were insufficient for estimating shear capacity with a fair level of precision. The CSA displayed the most accurate predictions among the four theories, while the ACI was the most cautious because it exhibited the most variability in the findings [19].

Reflecting on the preceding case study, the success of the algorithm in optimizing shear design is demonstrated by comparing its results with four widely used codes and standards. Furthermore, the algorithm's training with experimental data from the literature also proved the viability of the suggested model. A series of tests used to verify its results brought them closer to reality and added greater meaning to the findings. However, it would be preferable to include the schematic design of the concrete members (e.g., dimensions and reinforcing details), as well as providing examples that offer shear capacity values from experimental, codes, and the algorithm for clear comparison and further verification.

Resilient back-propagating neural network (RBPNN) in optimization of FRP

In this subsection, a case study from the literature is presented to discuss the use of resilient back-propagating neural network (RBPNN) machine learning to optimize the FRP used in retrofitting RC structures in shear. Abuodeh et al. (2020) [13] employed machine learning approaches to optimize the shear capacity of concrete beams bonded externally with FRP sheets. These machine learning techniques include the use of RBPNN as a regression tool, the neural interpretation diagram (NID), and the recursive feature elimination (RFE) algorithm to determine the factors that significantly affect the estimation of FRP shear resistance within the validated RBPNN, as shown in Figs. 34 and 35. Comparative studies were conducted with experimental data, as well as commonly used codes and standards, using statistical parameters for comparison terms such as root mean square error (RMSE), standard deviation (SD), coefficient of variation (COV), coefficient of determination (R^2), and mean predicted-to-experimental shear strength ratio ($\mu_{P:E}$). A parametric investigation was conducted, which was separated into two sections to explore the impact of FRP characteristics and stirrups (transverse reinforcement) on the FRP shear resistance. CFRP and GFRP composites were used in this study on both two sides bonded (SB) and U-shape wrapping (UW) FRP retrofitting systems. The findings of the research indicate that the FRP shear capacity could be predicted more precisely by the RBPNN using the chosen parameters from NID and RFE ($R^2 = 0.885$; RMSE = 8.1 kN) than by the RBPNN using the basic 15 parameters from the literature ($R^2 = 0.668$; RMSE = 16.6 kN). The RBPNN model exceeded the expectations of the following codes: FIB14 guidelines, CNR-DT 200 guidelines, and ACI 440.R-17 code in forecasting FRP shear capacity with the largest $R^2 = 0.961$ and the lowest RMSE = 9.4, SD = 8.8, COV = 28.6, and $\mu_{P:E} = 1.06$. As shown in Figs. 36 and 37, the correlation between the shear strength of FRP participation and the FRP sheet breadth-to-spacing ratio (W_f/S_f) rose marginally in slope, while the correlation between the FRP shear strength participation and the stirrups area-to-spacing ratio (A_v/S) grew considerably in slope when the retrofitting scheme for reinforced concrete beams strengthened with CFRP was transformed from SB to UW. For each FRP sheet thickness, there is an ideal breadth-to-spacing ratio (W_f/S_f) and an ideal stirrups area-to-spacing ratio (A_v/S) where the FRP shear strength participation (V_f) will not grow after that point. For both the SB and UW strengthening systems, this ideal ratio varied between 0.5 and 0.75. Using U-shape wrapping in both CFRP and GFRP sheets resulted in an additional vertical transition as a result of concrete containment and shear-flexure interaction that have been described in previous works, demonstrating the uniformity of the RBPNN with experimental studies [13].

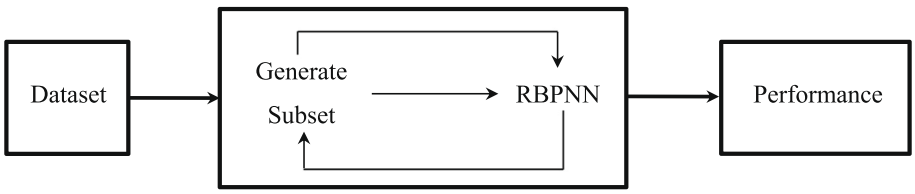

Fig. 34 RFE flow chart [13]

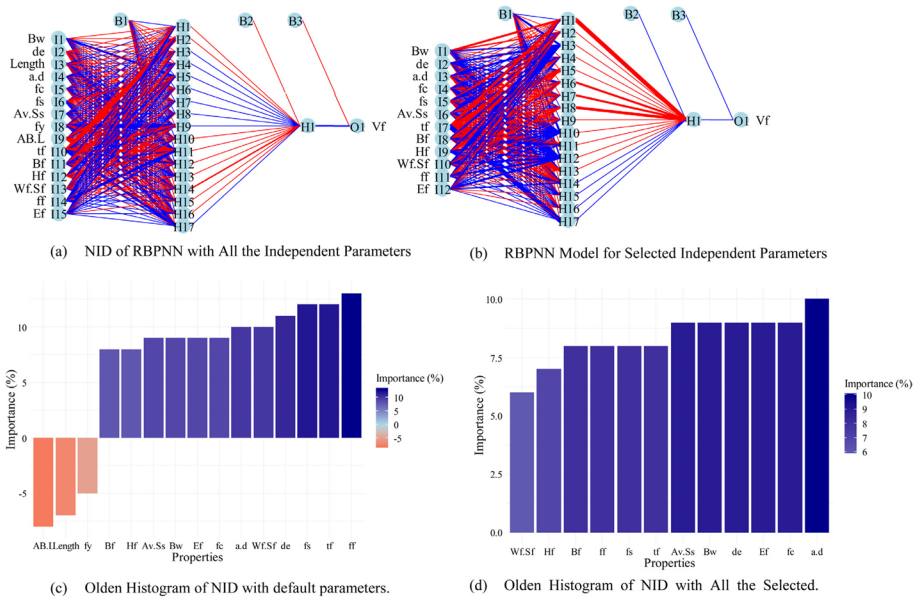

Fig. 35 **a** NID of RBPNN (all the independent parameters); **b** RBPNN Model (selected independent parameters) [13]

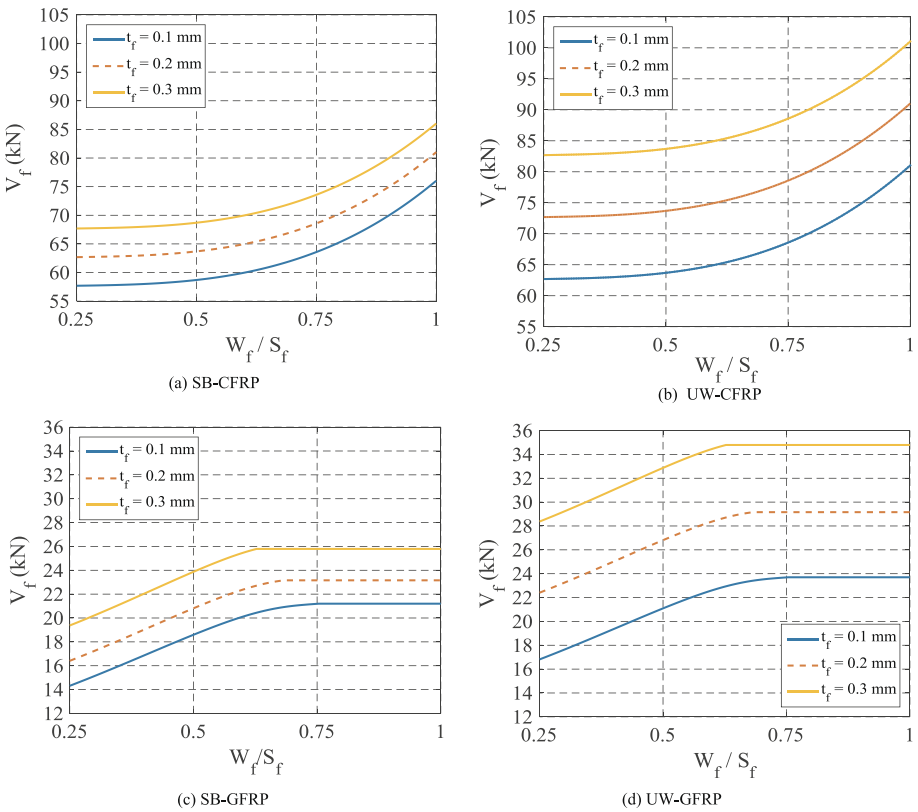

Fig. 36 Parametric study results for FRP properties effect. **a** SB-CFRP. **b** UW-CFRP. **c** SB-GFRP. **d** UW-GFRP [13]

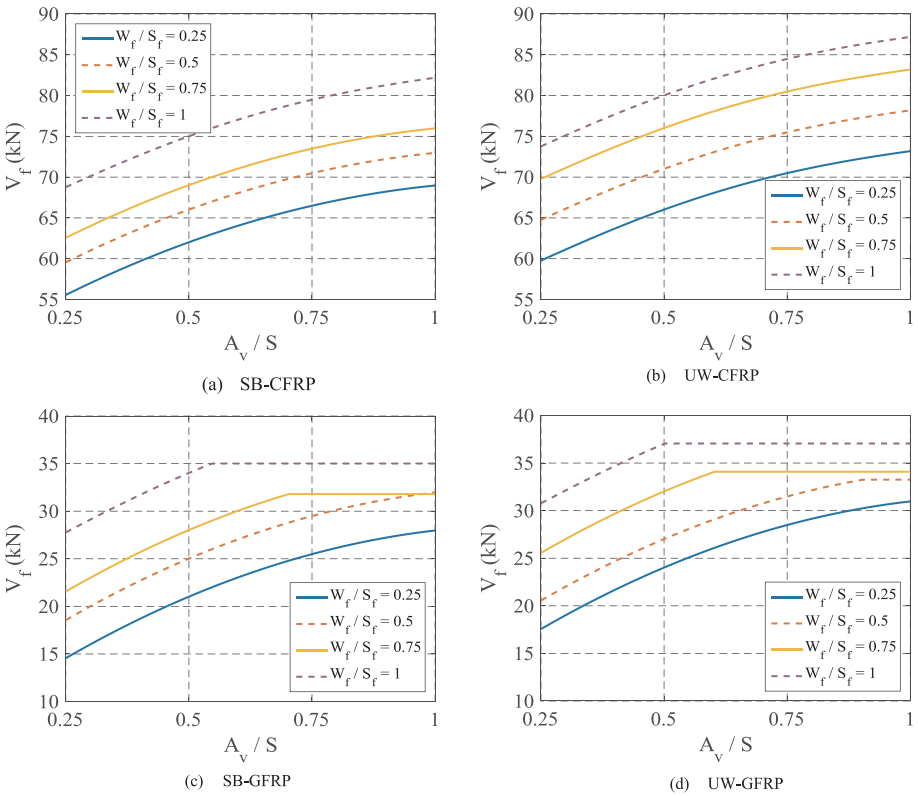

Fig. 37 Parametric study results for stirrups effect. **a** SB-CFRP. **b** UW-CFRP. **c** SB-GFRP. **d** UW-GFRP [13]

Discussing the prior case study, comparing the findings of the machine learning approaches with CNR-DT 200 guidelines, FIB14 guidelines, and ACI 440.R-17 code was beneficial, as it shows the success of these approaches in optimizing shear design. Additionally, the use of experimental data allows for the verification of the machine learning results, bringing them closer to reality and making them useful in real-world applications. However, it would be preferable to include the schematic configuration of the beams that shows the dimensions, reinforcing details, and FRP wrapping details, in addition to providing examples to offer the shear capacity from experimental, codes, and machine learning as values to facilitate comparison and for further verification.

Explainable single and ensemble models for machine learning techniques in optimization of FRP

In this subsection, various explainable single and ensemble machine learning models are presented through case studies from literature, compared against each other, to offer the best prediction for a particular application of FRP. Su et al. conducted a study in 2021 to predict the interfacial bonding strength (IBS) between FRP and concrete using three distinct machine learning (ML) methodologies: multiple linear regression (MLR), artificial neural network (ANN), and support vector machine (SVM). They utilized two datasets that contain the findings of a single-lap shear test for FRP sheets bonded externally to concrete prisms and to the grooves of concrete prisms. The externally bonded schemes are depicted in Fig. 38. Both datasets, compiled from literature (Fig. 39), were used to

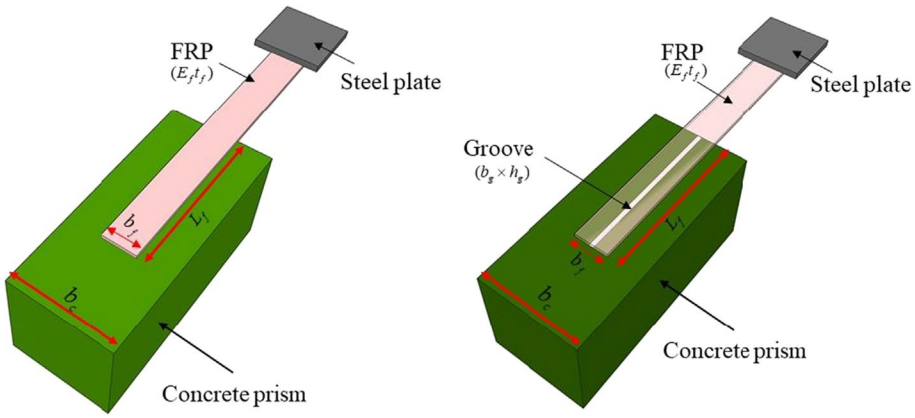

Fig. 38 Shear test. **a** Concrete externally bonded with FRP. **b** Concrete grooves externally bonded with FRP [35]

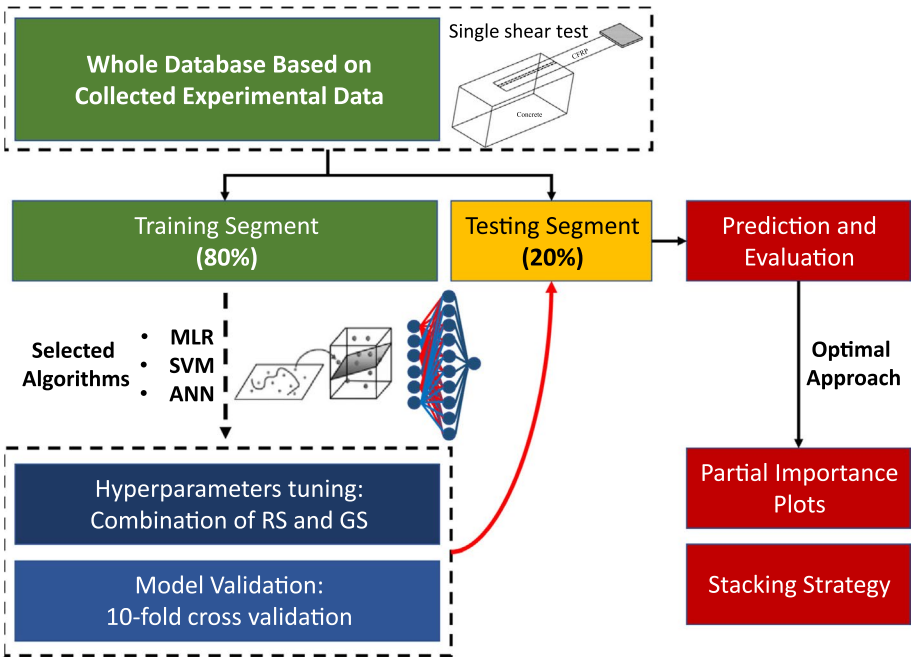

Fig. 39 ML model construction process [35]

train the three chosen ML techniques and evaluate their effectiveness. Dataset 1 had a set of 122 IBS data for FRP materials bonded externally to concrete, while Dataset 2 contained 136 IBS data for FRP materials bonded externally to concrete grooves. The precise of each ML model was evaluated in this study using the coefficient of determination R^2, mean absolute error (MAE), root mean square error (RMSE), and mean relative error (MRE). The ML techniques were compared with previous empirical IBS models. The findings showed that the SVM-ML approach had the most accurate and precise results for both datasets 1 and 2, as shown in Tables 18 and 19, respectively, in both training and testing the approach. In particular, Dataset 2 had higher prediction accuracy than Dataset 1. For dataset 1, the MLR-ML method exhibited the weakest predictive capability. However, for dataset 2, the prediction precision of the ANN and MLR were about

Table 18 For the training data, a comparison of the outcomes of 10-fold cross-validation [35]

Datasets	Methods	R^2	MAE	RMSE	MRE
Dataset 1	MLR	0.08	3.13	1.35	0.17
	SVM	0.82	1.39	0.96	0.11
	ANN	0.72	1.82	1.09	0.13
Dataset 2	MLR	0.88	1.30	1.01	0.09
	SVM	0.91	1.14	0.92	0.08
	ANN	0.88	1.34	1.01	0.09

Table 19 For the testing data, a comparison of the outcomes achieved using ML algorithms [35]

Datasets	Methods	R^2	MAE	RMSE	MRE
Dataset 1	MLR	0.74	1.22	1.88	0.13
	SVM	0.79	1.04	1.68	0.11
	ANN	0.77	1.18	1.76	0.12
Dataset 2	MLR	0.80	1.73	2.41	0.12
	SVM	0.85	1.41	2.08	0.09
	ANN	0.82	1.66	2.29	0.12

similar and not too significantly different from SVM-ML in the strategy's training, as shown in Table 18. The proposed SVM-ML technique exhibited the same or superior estimation efficiency on both datasets as compared to previous empirical IBS models, as displayed in Fig. 40 [35].

Analyzing the preceding case study using three ML approaches and comparing them based on IBS values from the literature was significant, as it resulted in more accurate and practical results. Additionally, the separation of the database into training and testing data was beneficial. Furthermore, comparing SVM-ML with the IBS empirical models was beneficial for verification purposes, as it shows the success of this approach. However, it would be better to provide an example indicating the IBS values from experimental and machine learning as values to facilitate the comparison and for clear verification.

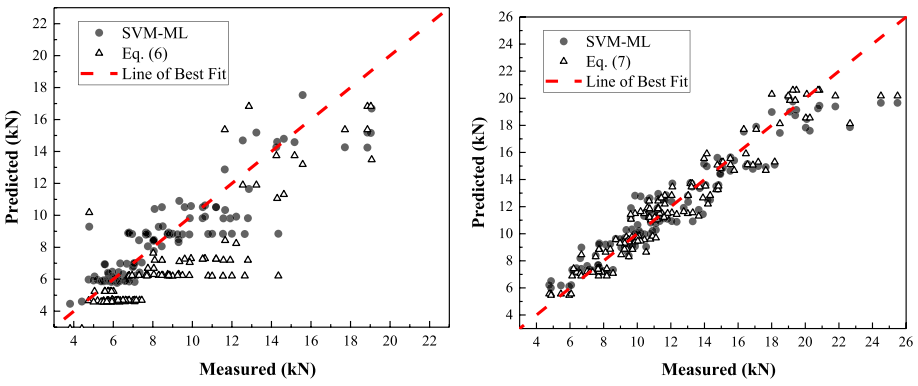

(a) Dataset 1 (b) Dataset 2

Fig. 40 SVM-ML and empirical models' comparison. **a** Dataset 1. **b** Dataset 2 [35]

Furthermore, in 2022, Tadesse G. Wakjira et al. developed research that utilized seven machine learning (ML) models for flexural-strengthened RC beams with innovative fabric-reinforced cementitious matrix (FRCM) composites to estimate the flexural capacities and loads. The seven machine learning models were divided into two categories: single AI models, which were K-nearest neighbors (KNN), support vector regression (SVR), kernel ridge regression (KRR), and decision trees (CART), while ensemble models were gradient-boosted trees (GBT), extreme gradient boosting (xgBoost), and random forest (RF). These models were compared and assessed to identify the ideal predictive model for FRCM-retrofitted beams. The unified Shapley Additive Explanations (SHAP) method was used to implement this evaluation. The conclusion of an optimal machine learning (ML) model was clarified using the unified SHAP methodology, and the majority of essential input characteristics and interactions that affect the flexural strength of FRCM-strengthened RC beams were pinpointed. A comparison between the suggested and current models was also conducted. The primary input parameters for the database were the geometry of the beams, the reinforcement area of FRCM, the reinforcement area of internal steel, and the mechanical properties of the concrete, steel, and FRCM. The provided database contains 132 RC beams that have been flexurally reinforced by FRCM. For the ML models, this database was split into teaching and validation datasets. The database took into account a wide variety of beam geometries (width ranging from 120 mm to 400 mm and depth ranging from 129 mm to 450 mm), FRCM fabric types (Polyparaphenylene Benzobisoxazole (PBO), carbon, and steel), mechanical properties of materials (concrete (f_c ranges from 15 to 68 MPa), FRCM (E_f ranges from 123 to 271 GPa), and steel (f_y ranges from 267 to 604 MPa)), and area of reinforcement for the external reinforcement of FRCM (A_f ranges from 7 mm^2 to 108 mm^2), and the internal reinforcement of steel (A_s ranges from 57 mm^2 to 603 mm^2 and A_s' ranges from 0 to 603 mm^2). According to the suggested xgBoost model, a design example of the FRCM retrofitting scheme for flexural-deteriorated RC beams was offered in the research (Fig. 41). The findings could be concluded as follows: with the lowest RMSE, MAPE, and MAE values as well as the greatest R^2 on both the teaching and validation datasets, the xgBoost model had the best forecasting performance. For the learning and trial datasets, the xgBoost model's R^2 value was 99.3% and 99.2%, respectively (Table 20). In addition, the comparative analysis between the suggested and current models demonstrated the significantly greater robustness and predictive ability of the suggested model. According to current models, the estimated load and flexural capacities of the retrofitted beams were very erratic and unsafe (Table 21). According to the findings of SHAP, the reinforcement area of FRCM, the reinforcement area of internal tensile steel, as well as the breadth and depth of the beam cross-section had the greatest impact on the retrofitted beams' flexural capacity [26].

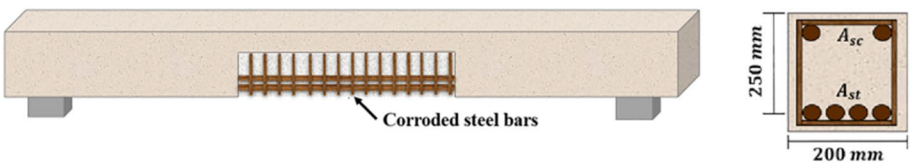

Fig. 41 Design example schematic and cross section details [26]

Table 20 ML models' performance metrics [26]

Model	Training dataset				Test dataset			
	RMSE (kN.m)	MAE (kN.m)	MAPE (%)	R^2(%)	RMSE (kN.m)	MAE (kN.m)	MAPE (%)	R^2(%)
KNN	4.80	3.10	5.87	97.2	8.43	5.15	9.30	93.1
KRR	4.45	3.56	7.86	97.6	4.71	3.37	7.32	97.8
SVR	3.97	2.72	5.77	98.1	4.44	3.04	6.01	98.1
CART	3.95	2.58	5.86	98.1	5.14	3.68	8.44	97.4
RF	3.71	2.67	5.52	98.4	4.30	3.51	7.92	98.2
GBT	2.52	1.84	3.91	99.2	3.19	2.33	4.73	99.0
xgBoost	2.41	1.55	3.17	99.3	2.70	1.77	3.25	99.3

Table 21 Existing and suggested models evaluation [26]

Model	Mean	STD	COV
Model-1	1.257	0.286	0.228
Model-2	0.738	0.134	0.182
Model-3	0.755	0.205	0.272
Model-4	0.799	0.162	0.203
Proposed xgBoost	1.002	0.048	0.048

STD Standard deviation, *COV* Coefficient of variation

Regarding the preceding case study, it was beneficial to split the database into learning and validation datasets to enhance the effectiveness of the machine learning models. Additionally, comparing seven distinct ML models to determine the best prediction model and then comparing the best model to the existing ones made the results more realistic and increased their reliability. Furthermore, the use of a novel and powerful ML technique, such as XGBoost, to evaluate an innovative strengthening technique, such as FRCM, along with the provision of a design example, is a unique advantage of the research.

As an extension of their research, Tadesse G. Wakjira et al. developed a study in 2022 that used six machine learning (ML) models to estimate the shear capacity of RC beams reinforced with innovative fabric-reinforced cementitious matrix (FRCM) composites. The six ML models used were support vector machine (SVR), decision trees (CART), gradient tree boosting (GTBR), random forest (RFR), extremely randomized trees (ERT), and extreme gradient boosting (xgBoost). These models were compared and assessed to identify the ideal predictive model for FRCM-retrofitted beams. A comparison analysis was performed between the suggested and current models. The provided database contained 173 FRCM-strengthened RC beams. For the ML models, this database was split into training and testing datasets. The database included a wide variety of beam geometries, concrete strengths, internal shear and flexural reinforcements, FRCM types, strengthening configurations, wrapping schemes, and mechanical properties of FRCM. Three types of wrapping schemes were used in the database: side bonded (SB) scheme, in which the FRCM was bonded to the two sides of the beam; U-wrapped (UW) scheme, in which the FRCM was applied to the bottom and two sides of the beam; and full wrapping

(FW) schemes, in which the FRCM composite was applied to the top, bottom, and two sides of the beam. In accordance with the suggested xgBoost model, the research offered a design example of a shear-strengthened beam with one layer of externally bonded U-wrapped steel FRCM reinforcement, as shown in Fig. 42 and Table 22. The following is a summary of the findings: The most effective approach for making consistent and precise predictions about the shear capacity of RC beams that have been strengthened with FRCM was the xgBoost model. For the training and test datasets, the experimental shear capacity and predicted values based on the xgBoost model exhibited the smallest error margins and the greatest correlation with coefficients of determination (R^2) of 0.995 and 0.984, respectively (see Table 23). Furthermore, the suggested xgBoost model provided safe and accurate predictions compared to all other current models. In comparison to the current models, the proposed xgBoost model significantly lowered the MAE and RMSE. For example, the comparable value for the suggested xgBoost model was 7.80 kN, which reflects a reduction in RMSE of 91%, 90%, 92%, 92%, 79%, and 85% compared to models 1, 2, 3, 4, and 5, respectively (see Table 24) [27].

Discussing the prior case study, after flexural retrofitting in the previous research, extending the research to evaluate an innovative strengthening technique, such as FRCM, with a cutting-edge and potent ML technique, such as xgBoost, for shear retrofitting was very advantageous and provided real evidence of the ability of the xgBoost technique. Another unique benefit of the research is the provision of a design example. To improve the efficiency of the machine learning models, the database was split into training and testing datasets. The results were also made more realistic and reliable by comparing the best model to the current models and then comparing it to the best prediction model among six other ML models.

Lastly, in 2022, Tadesse G. Wakjira et al. employed an optimized super-learner machine learning (ML) model to forecast the flexural capacity of FRP-RC beams. Gradient-boosted decision trees (GBDT), adaptive boosting (AdaBoost), classification and regression trees (CART), and extreme gradient boosting (XGBoost) were compared with the suggested super-learner ML model to demonstrate the approach's predictive ability. A comparison analysis between the suggested model and the current code and guideline

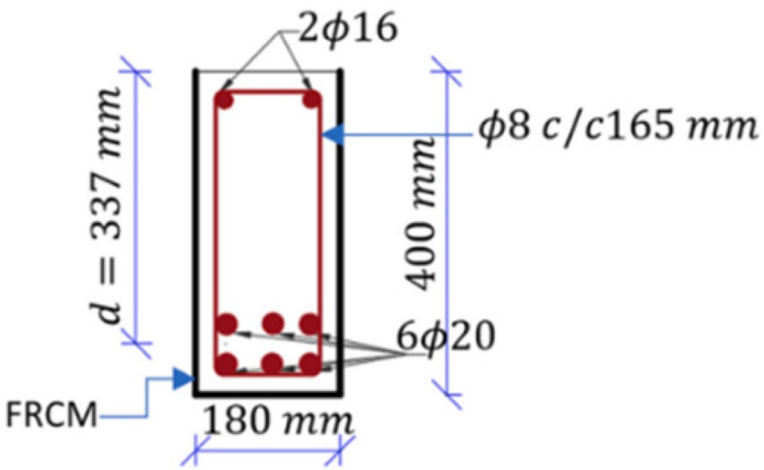

Fig. 42 FRCM-strengthened beam section [27]

Table 22 FRCM-strengthened beam design example

Internal reinforcement				FRCM properties						Resistance	
ρ_{sx}(%)	f_{sx}(MPa)	r_{sy}(%)	f_{sy}(MPa)	Fabric type	Wrapping scheme	t_f(mm)	n_f	ρ_f(%$_0$)	h_{fe}(mm)	V_n(kN)	φV_n(kN)
3.17	550	0.34	350	Steel	UW	0.084	1	0.933	297	197	179
3.17	550	0.34	350	Steel	UW	0.084	2	1.867	297	248	225
3.17	550	0.34	350	Steel	UW	0.169	2	3.756	297	290	263

Table 23 Performance metrics for the suggested models [27]

Models	Training dataset				Test dataset			
	MAPE (%)	MAE (kN)	RMSE (kN)	R^2	MAPE (%)	MAE (kN)	RMSE (kN)	R^2
SVR	6.69	7.97	14.55	0.968	10.01	13.76	19.29	0.952
CART	4.58	6.86	12.23	0.978	9.36	14.56	20 98	0.943
RFR	7.09	8.60	12.21	0.978	7.96	12.82	19.48	0.951
ERT	3.83	4.35	7.03	0.993	7.37	11.44	16.61	0.964
GTBR	3.50	4.30	6.78	0.993	8.48	10.50	13.55	0.976
xgBoost	1.84	2.62	5.94	0.995	6.16	8.23	10.96	0.984

Table 24 Performance of different shear models [27]

Model	Model ID	Sample size	RMSE (kN)	MAE (kN)	Mean of V_{pred}/V_{exp}	STD of V_{pred}/V_{exp}
Triantafillou and Papanicolaou	Model-1	173	87.02	65.30	1.28	0.81
Escrig et al.	Model-2	173	81.60	60.66	0.66	0.26
Ombres	Model-3	95	97.17	73.86	0.53	0.25
ACI 549.4R	Model-4	95	97.21	77.83	0.49	0.21
Wakjira and Ebead	Model-5	128	37.84	27.97	0.94	0.22
Wakjira and Ebead	Model-6	128	50.29	37.60	0.90	0.28
xgBoost	–	173	7.80	4.30	0.99	0.06

STD Standard deviation

equations ACI 440.1R-15 and CAN/CSA-S806-12 was performed. The researchers assembled 132 experimental datasets on the flexural strength of FRP-RC beams and randomly divide them into 80% learning datasets and 20% validation datasets. The primary parameters included in the database were the effective depth and width of the beam, flexural reinforcement ratio of FRP, concrete compressive strength, ultimate tensile strength of FRP, and modulus of elasticity of FRP. The database comprised four different types of FRP composites: BFRP, CFRP, GFRP, and AFRP. The super-learner model utilized linear support vector regression (SVR) as a meta-model to integrate the AdaBoost, CART, and GBDT as basic learner models into a robust, individual model (see Fig. 43).

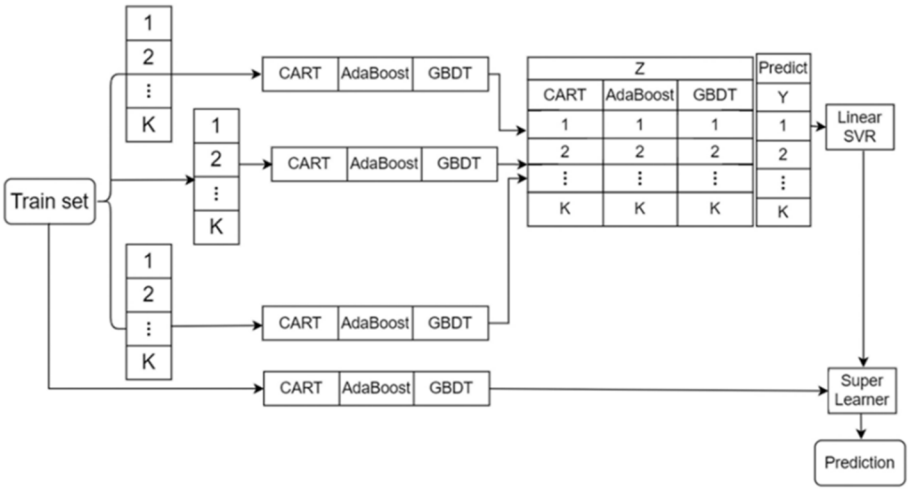

Fig. 43 Super-learner model training process [9]

The constructed super-learner model was employed to establish a smart forecasting tool for the computing of the flexural strength of FRP-RC beams, which can be used on any device, such as a computer, tablet, or phone. The graphical user interface (GUI) of the created web-based estimation tool is displayed in Fig. 44. The study found that the ability of all ensemble models to forecast the flexural strength of FRP-RC beams was remarkable. The behavior of the super-learner model was superior to that of the boosting ensemble techniques (GBDT, AdaBoost, and XGBoost). The super-learner model offered the greatest forecasting accuracy with the lowest RMSE and MAPE, as well as the highest R^2 of all the models examined in this study (see Table 25). In comparison to the CAN/CSA-S806-12 and ACI 440.1R-15 equations, the suggested model had a higher ability to forecast the flexural capacity of FRP-RC beams, according to the comparative analysis (see Table 26) [9].

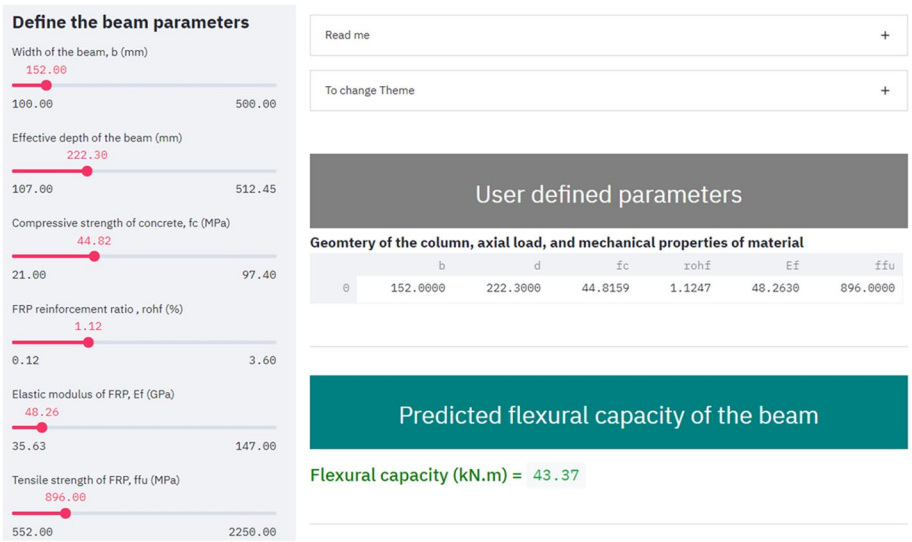

Fig. 44 Web-based prediction tool's graphical user interface (GUI) [9]

Table 25 ML models performance indices [9]

Models	Training set			Test set		
	MAPE (%)	RMSE (kN.m)	R^2(%)	MAPE (%)	RMSE (kN.m)	R^2(%)
CART	8.54	5.83	98.5	20.77	20.91	83.5
AdaBoost	4.96	3.10	99.6	8.96	6.91	98.2
GBDT	1.84	1.39	99.9	8.12	6.37	98.5
XGBoost	1.44	0.80	100	7.33	6.33	98.5
Super-learner	1.82	1.61	99.9	6.63	5.61	98.8

Table 26 Existing vs Super-learner models [9]

Model	MAPE (%)	RMSE (kN•m)	R^2 (%)
ACI 440.1R-15	21.81	16.15	88.64
CAN/CSA-S806-12	25.87	19.84	82.85
Super-learner	3.37	2.91	99.63

Analyzing the preceding case study, it was advantageous to split the database into learning and validation datasets for the purpose of maximizing the behavior of the super-learner machine learning (ML) model. Comparing the suggested model to four distinct machine learning (ML) models and then comparing it to the CAN/CSA-S806-12 and ACI 440.1R-15 equations made the results more accurate and improved their dependability. This also clarified the estimation accuracy of the super-learner ML model. Additionally, the utilization of a powerful ML technique, such as a super-learner model that integrates cutting-edge ML techniques like CART, AdaBoost, and GBDT as basic learner models with linear support vector regression (SVR) as a meta-model, was also very beneficial. It provided an entirely novel approach to employing ML techniques. A superior practical application for the super-learner machine learning (ML) model was the creation of an intelligent web-based prediction tool with a simplified graphical user interface (GUI). However, it was desirable to compare the super-learner machine model with additional existing codes and guidelines to make the comparison more evident and to provide more verification of the model's performance.

Discussion

The previous case studies, which showcase the most common FRP applications and different optimization algorithms and machine learning techniques applied in optimizing FRP, are summarized in Table 27:

The genetic algorithm was the most widely used algorithm, accounting for 50% of all usage in this study's research, followed by machine learning approaches (35%) and particle swarm optimization (15%). On the other hand, the algorithms and machine learning methods employed in FRP applications in shear account for 45%, followed by flexure (25%), seismic (15%), and other prediction purposes (15%) (Figs. 45 and 46).

The genetic algorithm (GA) is an optimal algorithm, which makes it easy to use in half of the cases discussed in this research. It also has the capacity to be used in many different contexts, such as shear, flexure, seismic, and corrosion. In addition, case studies were carried out by M. Nehdi et al. in 2007, Nehdi and Nikopour in 2010, Ebid and Deifalla in 2021, and Abathar Al-Hamrani et al. in 2023 to verify the algorithmic results with experimental results and compare them to code results. These studies show that the algorithmic results have good agreement with the experimental results and are also superior to the code results. Furthermore, research by Ebid and Deifalla in 2021 indicates that when an algorithm is trained on experimental results before being tested on different experimental findings, the results are more accurate and precise. Perera and Varona's 2009 research demonstrates the flexibility of the algorithm to incorporate different models, such as the Jansze 1997 model and the Matthys 2000 model. Additionally, as demonstrated by Chisari and Bedon in 2016, 2017, and Mahdavi et al. in 2019, the algorithm has the ability to produce non-uniform outcomes for the same elements in order to achieve the best solution. For example, it can use different thicknesses for the internal and external columns, considering their floors. Out of all the case studies mentioned, the one performed by Ebid and Deifalla in 2021 is the most successful approach

Table 27 Summary of cases

Algorithm/ML	FRP application	Reference	Case study	Objective function	Constrains
GA	Shear and flexure	[31]	RC Beam	Minimize cost	Codes
GA	Shear and flexure	[32]	RC Beam	Minimize cost	Codes
GA	Shear	[17]	RC Beam	Optimize capacity	Experimental laboratory test
GA	Shear	[7]	RC Beam	Optimize capacity	Experimental laboratory test
GA and multi-objective	Seismic	[10]	RC Frame	Minimize cost/maximize ductility	FE model
GA and multi-objective	Seismic	[11]	RC Frame	Minimize cost/maximize ductility	Damage levels
GA	Corrosion	[33]	RC Column	Strengthening time/number of FRP layers	Time-dependent reliability method Renewal theory
GP	Shear	[8]	RC Beam	Optimize capacity	Experimental laboratory test
GA	Shear	[20]	RC Slab	Optimize capacity	Experimental laboratory test
PSO	Flexure	[18]	RC Beam	Minimize cost	Codes
PSO and multi-objective	S.H.M	[34]	RC Beam	Minimize error	Numerical models, Experimental tests
GA and PSO	Seismic	[12]	RC Frame	Minimize FRP/maximize resiliency	Plastic hinge rotation capacity
GRNN	Shear	[19]	RC member	Optimize capacity	Experimental laboratory test
RBPNN	Shear	[13]	RC Beam	Optimize capacity	Experimental laboratory test
MLR, SVM and ANN	Bond Strength	[35]	RC member	Interfacial bond strength	Empirical IBS models
KRR, KNN, SVR, CART, RF, and GBT and xgBoost	Flexure	[26]	RC Beam	Optimize capacity	Experimental laboratory test
SVR, CART, and RFR, and ERT, GTBR and xgBoost	Shear	[27]	RC Beam	Optimize capacity	Experimental laboratory test
Super-learner	Flexure	[9]	RC Beam	Optimize capacity	Experimental laboratory test

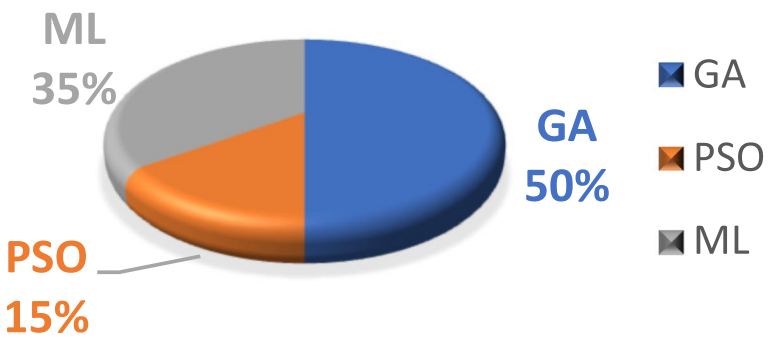

Fig. 45 Optimization techniques usage

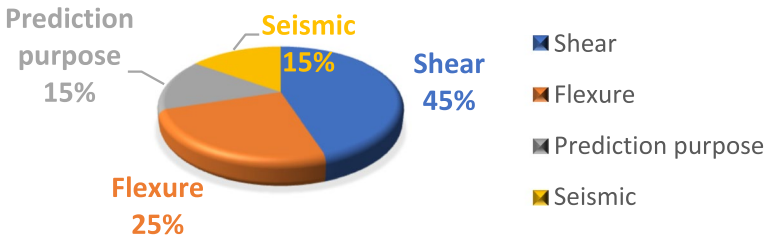

Fig. 46 FRP applications usage

that uses genetic algorithms (GAs). This study demonstrates the success of the algorithm when training and testing with experimental results and comparing them with codes to prove the good agreement with experimental results over the code results. Additionally, it offers schematic design details for concrete and FRP.

Several case studies, such as those by M. Nehdi et al. in 2007, Nehdi and Nikopour in 2010, Perera et al. in 2014, Alam and Gazder in 2019, Abuodeh et al. in 2020, Su et al. in 2021, Ebid and Deifalla in 2021, Tadesse G. Wakjira et al. in 2022, and Abathar Al-Hamrani et al. in 2023, use experimental data to verify and demonstrate the effectiveness of algorithms or machine learning techniques, such as GA, PSO, GRNN, RBPNN, SVM, xgBoost, and super-learner. On the other hand, various case studies do not show the usefulness of algorithms, such as Perera and Varona in 2007, 2009, INNOCENTE et al. in 2007, Chisari and Bedon in 2016, 2017, Baji et al. in 2018, and Mahdavi et al. in 2019. Additionally, some case studies train and test algorithms or machine learning techniques, such as GA, GRNN, SVM, xgBoost, and super-learner, to provide findings that align with experimental data, making the results more realistic and applicable to real-world applications. Examples of these studies include Nehdi and Nikopour in 2010, Alam and Gazder in 2019, Su et al. in 2021, Ebid and Deifalla in 2021, and Tadesse G. Wakjira et al. in 2022. Furthermore, case studies demonstrate that widely used codes, such as ACI, CSA, JSCE, ISIS, and Eurocode, tend to be more conservative in their results when compared to experimental findings. Examples of these studies include M. Nehdi et al. in 2007, Nehdi and Nikopour in 2010, Alam and Gazder in 2019, Abuodeh et al. in 2020, Ebid and Deifalla in 2021, Tadesse G. Wakjira et al. in 2022, and Abathar Al-Hamrani et al. in 2023. Moreover, some case studies involving the use of FRP in retrofitting demonstrate the effectiveness of the material by comparing the outcomes before and after the retrofit. Examples of these studies include Perera and Varona in 2007, Chisari and Bedon in 2017, Baji et al. in 2018, and Mahdavi et al. in 2019. However, other cases do not demonstrate the efficacy of the FRP, such as Perera and Varona in 2009, Nehdi and Nikopour in 2010, Chisari and Bedon in 2016, and Abuodeh et al. in 2020.

Conclusions

Optimization algorithms and machine learning techniques can be used to optimize FRP applications in the design and strengthening of RC structures for shear, flexure, and seismic forces. These techniques can also be used for other purposes such as structure health monitoring, corrosion deterioration prediction, and calculation of bond strength

between FRP and concrete. The overall aim of this research is to critically review case studies from the literature in order to determine the optimal algorithm or machine learning technique for optimizing FRP applications based on the investigated case studies. The 18 case studies selected to approximately reflect the most common FRP applications and various algorithms and machine learning techniques used in optimizing FRP are discussed and critically appraised.

The genetic algorithm (GA) is an optimal algorithm that is employed in half of the cases discussed in this research and can be applied to a variety of applications, such as shear, flexure, seismic, and corrosion. Some case studies analyze and compare the results of the codes and the algorithm, showing that the algorithm's results outperform the codes' results and have strong agreement with the experimental data. The algorithm's results are more precise when it is trained on experimental data before being tested against other experimental findings. In addition, various case studies prove the effectiveness of GA, PSO, GRNN, RBPNN, SVM, xgBoost, and super-learner by using experimental data for verification. Furthermore, GA, GRNN, SVM, xgBoost, and super-learner were trained and tested using the experimental data, producing good agreement and realistic results. Moreover, other case studies show that, when compared to experimental results, the most prevalent codes, such as ACI, CSA, JSCE, ISIS, and Eurocode, are more conservative in their conclusions. Regarding the case studies concerning the usage of FRP in retrofitting, some cases illustrate the material's efficiency by contrasting the results before and after the retrofit, but other cases do not. Finally, this research outlines the optimal optimization algorithm for optimizing FRP applications in designing and retrofitting RC structures, which is the genetic algorithm (GA). Furthermore, it presents a detailed analysis of the various optimization strategies used and their findings to present the benefits and drawbacks of the mentioned optimization techniques. It also provides illustrations of the desired conditions that are recommended to be investigated so that future researchers and specialists can use this research as a reference.

Recommendations and future work

This research presents the following recommendations: Based on the studied cases, machine learning methods such as GRNN, RBPNN, SVM, xgBoost, and Super-learner are recommended to be investigated for more cases involving the design and retrofitting of RC members with FRP. Other optimization approaches and algorithms, such as the simulated annealing method (SA), reliability-based design optimization (RBDO), and ant colony optimization (ACO), are also worth investigating as it is possible to correlate them with the previously implemented algorithms in order to achieve the most effective and reliable techniques for optimizing FRP applications. Additionally, it is significant to conduct an investigation into the application of optimization techniques in optimizing FRP-reinforced or strengthened piles, as very limited research has been performed for FRP-reinforced or strengthened piles. For FRP-strengthened RC members, limited studies have been conducted on FRP retrofitting for flexure design, particularly in comparison to shear design, which has been extensively studied. It is fundamental to conduct more research on flexure design.

Limitations

Although the case studies mentioned in this research cover the most prevalent FRP applications, as well as various algorithms and machine learning techniques utilized in optimizing FRP for the categories described above, some cases were not explored in this study due to time constraints and to prevent an increase in research length, which makes full familiarity with all case studies difficult. For the seismic category, case studies from the last 6 years were reviewed, while for other prediction purposes, case studies from the last 8 years were reviewed. It is worth investigating other research in order to provide more comparisons and verification.

Acknowledgements
The author would like to express appreciation to Dr. Elbadr M. Osman (AASTMT) for his assistance and efforts in carrying out this research, as well as Dr. Alaa M. Morsy (AASTMT) for his inspiration for the FRP strengthening idea.

Authors' contributions
All authors read and approved the final manuscript.

Funding
No financial support was received for this study.

Availability of data and materials
The authors declare that all data supporting the study's findings are included within the article and the cited references which are listed in the references section.

Declarations

Competing interests
The authors declare that they have no competing interests.

Received: 9 January 2023 Accepted: 29 April 2023
Published online: 21 June 2023

References

1. Buchan PA, Chen JF (2007) Blast resistance of FRP composites and polymer strengthened concrete and masonry structures – a state-of-the-art review. Compos B Eng 38(5–6):509–522
2. Falcone R et al (2019) Seismic retrofitting of existing RC buildings: a rational selection procedure based on Genetic Algorithms. Structures 22:310–326
3. Banayan-Kermani A, Bargi K, Heidary-Torkamani H (2016) Seismic performance assessment of pile-supported wharves retrofitted by carbon fibre–reinforced polymer composite considering ageing effect. Adv Struct Eng 19(4):581–598
4. Ibrahim M, Wakjira T, Ebead U (2020) Shear strengthening of reinforced concrete deep beams using near-surface mounted hybrid carbon/glass fibre reinforced polymer strips. Eng Struct 210:110412
5. Najaf E, Orouji M, Ghouchani K (2022) Finite element analysis of the effect of type, number, and installation angle of FRP sheets on improving the flexural strength of concrete beams. Case Stud Constr Mater 17:e01670
6. Aydın E, Boru E, Aydın F (2021) Effects of FRP bar type and fiber reinforced concrete on the flexural behavior of hybrid beams. Constr Build Mater 279:122407
7. Nehdi M, Nikopour H (2010) Genetic algorithm model for shear capacity of RC beams reinforced with externally bonded FRP. Mater Struct 44(7):1249–1258
8. Ebid AM, Deifalla A (2021) Prediction of shear strength of FRP reinforced beams with and without stirrups using (GP) technique. Ain Shams Eng J 12(3):2493–2510
9. Wakjira TG et al (2022) FAI: fast, accurate, and intelligent approach and prediction tool for flexural capacity of FRP-RC beams based on super-learner machine learning model. Mater Today Commun 33:104461
10. Chisari C, Bedon C (2016) Multi-objective optimization of FRP jackets for improving the seismic response of reinforced concrete frames. Am J Eng Appl Sci 9(3):669–679
11. Chisari C, Bedon C (2017) Performance-based design of FRP retrofitting of existing RC frames by means of multi-objective optimisation. Boll Geofis Teor Appl 58:377–394
12. Mahdavi G, Nasrollahzadeh K, Hariri-Ardebili MA (2019) Optimal FRP jacket placement in RC frame structures towards a resilient seismic design. Sustainability 11(24):6985
13. Abuodeh OR, Abdalla JA, Hawileh RA (2020) Prediction of shear strength and behavior of RC beams strengthened with externally bonded FRP sheets using machine learning techniques. Compos Struct 234:111698
14. Tahzeeb R, Alam M, Muddassir SM (2022) A comparative performance of columns: reinforced concrete, composite, and composite with partial C-FRP wrapping under contact blast. Mater Today Proc 62:2191–2202
15. Saribiyik A, Abodan B, Balci MT (2021) Experimental study on shear strengthening of RC beams with basalt FRP strips using different wrapping methods. Eng Sci Technol Int J 24(1):192–204

16. Zhang SS et al (2022) Effect of load distribution on the behaviour of RC beams strengthened in flexure with near-surface mounted (NSM) FRP. Compos Struct 279:114782
17. Nehdi M, El Chabib H, AlySaïd A (2007) Proposed shear design equations for FRP-reinforced concrete beams based on genetic algorithms approach. J Mater Civil Eng 19(12):1033–42
18. Innocente MS, et al (2007) Optimal flexural design of frp-reinforced concrete beams using a particle swarm optimizer. In: FRPRCS-8: 8th International Symposium on Fiber Reinforced Polymer Reinforcement for Reinforced Concrete Structures. Patras. https://doi.org/10.48550/arXiv.2101.09974
19. Alam MS, Gazder U (2019) Shear strength prediction of FRP reinforced concrete members using generalized regression neural network. Neural Comput Appl 32(10):6151–6158
20. Al-Hamrani A et al (2023) Sensitivity analysis and genetic algorithm-based shear capacity model for basalt FRC one-way slabs reinforced with BFRP bars. Compos Struct 305:116473
21. Han S et al (2023) Shear behavior of concrete beams reinforced with corrosion-resistant and ductile longitudinal steel-FRP composite bars and FRP stirrups. Eng Struct 278:115520
22. Zeng J-J et al (2023) Behaviour of FRP spiral-confined concrete and contribution of FRP longitudinal bars in FRP-RC columns under axial compression. Eng Struct 281:115747
23. Alwan GM (2016) OptimizationTechnique
24. Dede T, Kripka M, Togan V, Yepes V, Rao RV (2019) Usage of optimization techniques in civil engineering during the last two decades. Curr Trends Civil Struct Eng 2(1):1–17
25. Shahnewaz M et al (2016) Optimized shear design equation for slender concrete beams reinforced with FRP bars and stirrups using Genetic Algorithm and reliability analysis. Eng Struct 107:151–165
26. Wakjira TG et al (2022) Explainable machine learning model and reliability analysis for flexural capacity prediction of RC beams strengthened in flexure with FRCM. Eng Struct 255:113903
27. Wakjira TG, Ebead U, Alam MS (2022) Machine learning-based shear capacity prediction and reliability analysis of shear-critical RC beams strengthened with inorganic composites. Case Stud Constr Mater 16:e01008
28. Truong GT, Hwang H-J, Kim C-S (2022) Assessment of punching shear strength of FRP-RC slab-column connections using machine learning algorithms. Eng Struct 255:113898
29. Zhang S-Y et al (2022) Data-driven prediction of FRP strengthened reinforced concrete beam capacity based on interpretable ensemble learning algorithms. Structures 43:860–877
30. Zhang F et al (2023) Prediction of FRP-concrete interfacial bond strength based on machine learning. Eng Struct 274:115156
31. Perera R, Varona FB (2007) Design of frp laminates using evolutionary algorithms. In: FRPRCS-8: 8th International Symposium on Fiber Reinforced Polymer Reinforcement for Reinforced Concrete Structures. Patras. http://hdl.handle.net/10045/8150
32. Perera R, Varona FB (2009) Flexural and shear design of FRP plated rc structures using a genetic algorithm. J Struct Eng 135(11):1418–29
33. Baji H, Yang W, Li C-Q (2018) Optimal FRP-strengthening strategy for corrosion-affected reinforced concrete columns. Struct Infrastruct Eng 14(12):1586–1597
34. Perera R et al (2014) Identification of intermediate debonding damage in FRP-plated RC beams based on multi-objective particle swarm optimization without updated baseline model. Compos B Eng 62:205–217
35. Su M et al (2021) Selected machine learning approaches for predicting the interfacial bond strength between FRPs and concrete. Constr Build Mater 270:121456

Publisher's Note